LAPPEENRANTA UNIVERSITY OF TECHNOLOGY
Faculty of Technology
Degree Program in Technical Physics

Kostiantyn Nechay

Interferometric multichip VECSEL

Examiners: Academy Postdoctoral researcher Esa J. Saarinen
Professor Erkki Lahderanta

Abstract

Kostiantyn Nechay

Master's Thesis
2016

LAPPEENRANTA UNIVERSITY OF TECHNOLOGY
Faculty of Technology
Master degree Programme in Technical Physics

Interferometric multichip VECSEL

74 pages, 54 figures

Examiners: Academy Postdoctoral Researcher Esa J. Saarinen
Professor Erkki Lahderanta

Keywords:

VECSEL, interferometry, coherent combining, single-frequency, power scaling, Michelson interferometer, Fabry-Perot interferometer, optical pumping, semiconductor, beam splitter.

Lasers with narrow optical spectrum linewidth, tunable operational wavelength and multiwatt output powers are highly demanded and have a lot of fields to be applied at. This work is focused on a passive intracavity frequency mode selection technique of a laser light. Frequency mode selection is implemented by means of Michelson-type interferometric laser design. Frequency selectivity of the multichip laser can be controlled by changing the optical cavity length. Two *optically pumped semiconductor vertical external cavity surface emitting laser* (OPS-VECSELs) have been coherently combined with this method for the first time.
This thesis includes detailed explanations of the design, setting up and alignment of the interferometric multichip VECSEL.
The experimental laser setup has been scrutinized and spectral, spatial and power characteristics have been presented. Frequency selection with the interferometric frequency mode suppression technique has been demonstrated. Frequency selection resulted in narrowing of the optical spectrum linewidth from 10 to 1 nm. Problematics of the interferometric laser, such as instability due to vibrations and VECSEL chip selection, have been discussed. Attempts to improve the setup, by means of placing the laser into an isolating box for decreasing the mechanical and acoustic vibrations, have been. The suggestions for the improving and optimizing of the setup have been proposed. Stable and optimized VECSEL with the narrower optical linewidth can be frequency doubled for the further numerous applications: in medical field for an activating the drugs inside a human body; in imaging field, it can be used as a source of red light; in spectroscopy field, it can be an investigative tool for high-resolution spectroscopy measurements.

Acknowledgements

The work presented has been carried out on the base of Optoelectronic Research Centre (ORC) of Tampere University of Technology.Thus, I want to send my deepest appreciation to Head of the Department, Pekka Savolainen, for providing me the singular opportunity to be a part of the greatest scientific community, which made this the best period in my life.

The person, without whom this Master thesis would not exist, is Academy Postdoctoral Researcher Esa J. Saarinen. I would like to express my greatness gratitude to Esa Saarinen for all his efforts and time spent on this work, also for his exceptional ability to explain and inspire, for his desire to share the knowledge, for his infiniteness care and concern about the thesis and work. Thank you very much for being the best mentor one can ever dream about!

My considerable appreciation goes to Professor Erkki Lahderanta, for his valuable support and encouraging during studying in the University and throughout the Master thesis writing. In his face, I would like to thank Lappeenranta University of Technology. LUT represents the example of high quality, progressive and modern educational system unit, which is built and rely on the professors such as Erkki Lahderanta.

I would like to say thanks to Oleg Okhotnikov, may he rest in peace, for taking me as his Master thesis student at the ORC.

I have to express my appreciation to all people by whom I have been surrounded during my work on Master thesis in ORC. Anne Viherkoski deserves many thanks for the help, for her care and attention she paid on me regarding all administrative issues. Eija Heliniemi was always very kind and responsive, assisting with all issues concerning the work during my time in ORC. Colleagues: Antti Saarela, Teppo Noronen, Joona Rissanen, Mikhail Alimbekov helped me a lot by teaching me the basics of the laboratory work issues, thank you all.

My family deserves the biggest and warmest appreciation for all the support, faith and help they gave to me during my studies abroad. It would not possible even to think about the completion the Master degree without them.

Finally yet importantly, I would like to thank Finland and its citizens for all years spent here, for providing the opportunity to study here, for the warm hospitability and for the unforgettable memories!

Contents

List of abbreviations and symbols

Abbreviations

AC	Alternative current
AlGaAs	Aluminum-Gallium-Arsenide
AR	Anti-reflective
BS	Beam splitter
CO_2	Carbon dioxide
CD	Compact disk
COIL	Chemical oxygen iodine laser
DBR	Distributed Bragg reflector
DC	Direct current
DFB	Distributed feedback
FEL	Free-electron laser
GaAs	Gallium-Arsenide
HR	High-reflective
InGaAs,	Induim-Gallium-Arsenide
InP	Indium-Phosphide
IR	Infrared
LIGO	Laser Interferometer Gravitational-Wave Observatory
OC	Output coupler
OPSDL	Optically pumped semiconductor disk laser
QW	Quantum well
RF	Radio Frequency
RPG	Resonant periodic gain
SESAM	Semiconductor Saturable absorber mirror
SHG	Second-harmonic generation
TEC	Thermoelectric cooling
UV	Ultraviolet
VCSEL	Vertical cavity surface emitting laser
VECSEL	Vertical external cavity surface emitting laser
VR	Virtual reality

Symbols

T_c	Beam splitter transmission coefficient
τ_c	Coherence time
c	Speed of light
L	Optical path length
l	Coherence length
n	Refractive index
q	Distance between transmission peaks
R	Fiber ring radius
V	Speed of Earth
ΔL	Difference in interferometer arm's length
$\Delta\omega$	Bandwidth
ν	Frequency
ω	Angular velocity

Chapter 1

Introduction

1.1 Laser world

No one will deny the importance of the invention of laser made by T. Maiman in 1960 [1]. During the next 56 years the principle of laser has been unstoppably expanding into numerous laser types and families giving a possibility to discover more and more fruitful applications. Even after such a long period of modernizations, improvements and inventions of new lasers, this field is still dynamically developing.

Acronym *light amplification by stimulated emission of radiation* (laser) has become a common noun and has deeply penetrated into culture and everyday life for the past half a century. Science fiction writers received a new scientific device, which they put in arms of intergalactic soldiers as a weapon, doctors obtained an instrument that allowed them to put surgery to a new level, scientists gained a new powerful tool which metaphorically and literally showed the way for further great and revolutionary inventions in countless fields of technology and science.

The importance of laser technologies can be shown by examining laser applications in everyday life. One can make a thought experiment of a person dealing with lasers and laser-based technologies during one day. The imaginary Mr. Citizen wakes up in the morning and makes tea. In order to have water heated up to a proper temperature, Mr. Citizen measures the kettle temperature using a pyrometer equipped with a laser diode

pointer. Mr. Citizen cannot imagine drinking tea without lemon, and cuts a lemon with a knife, manufactured by using carbon dioxide laser cutting [2]. Later that day Mr. Citizen has an appointment with an ophthalmologist for laser vision correction by means of an ultraviolet excimer laser [3]. After that Mr. Citizen buys a music disk, scanned at the cashier by a laser barcode reader. At the end of the day, Mr. Citizen listens to music using a CD-player where an AlGaAs laser reads the information from the CD [4]. Being a music fan, Mr. Citizen considers it his duty to write a review about the CD. Thus, he sends an electronical review using the Web. His review reaches the neighboring continent by travelling through optical fibers laid on the ocean floor, where data are encoded and have a form of light pulses generated by an infrared laser [5]. The examples mentioned above concern only a tiny part of civil applications of laser technologies. However, this demonstrates that laser technologies are an integral part of the modern life. As the latest invention in the high technology field, the laser-based detectors can mentioned, which allow the user be fully integrated into the virtual reality, using his body both as an input device and as a main tool of interaction with virtual reality environment [6].

Since its invention, lasers have been ubiquitously popularized in science-fiction literature, fixedly associated with the space and synonymized as a weapon of future wars. In spite of fiction style of the literature, the truth is not far at all from the ideas described in sci-fi. The megawatt class chemical oxygen iodine laser (COIL) has proved itself as a powerful weapon system for missile defense [7]. The first space projects involving lasers date back to 1980s [8]. Space-based laser research covers topics ranging from an orbital solar power station which transmits the power by lasers to the Earth [9] to laser-based propulsion systems for making space travels easier and faster [10], and projects concerning a planetary defense system, which literally can save the entire life on Earth from asteroid threat [11]. The above-mentioned examples of already available laser-based technologies as well as examples of technologies researched and prepared for further implementation, serve as a solid proof of the fact that lasers and laser-based technologies are currently an integral and crucial part of modern science and technology and will remain so during next centuries.

1.2 Description of the work

Lasers play a seminal role also in this work. The thesis focuses on frequency selection and power scaling of the laser output, which is implemented by means of an interferometric technique, which in theory, allows not only achieving single-frequency operational regime, but also enables combining multiple chips in one interferometric setup. Single-frequency lasers are demanded in many fields: high-resolution spectroscopy, second-harmonic generation for obtaining visible light and optoelectronic communications. The laser investigated in this thesis is the optically pumped semiconductor vertical-external cavity surface emitting laser (OPS VECSEL). VECSELs have proved themselves as a multifunctional and balanced laser type. In sum, all these features create a desire for an interferometrically enhanced multiwatt single-frequency VECSEL.

The remarkable feature of this work is that it presents a combination of two phenomena: light interference and stimulated emission. As a result, a merger of two devices based upon these concepts, the previously mentioned VECSEL and Michelson interferometer, is shown. It is worth mentioning that the time delay between the first demonstrations of these two devices is equal to more than 100 years! In the author's opinion, the fact of combining old and new techniques and devices is an evidence of progress, since the new invention brings impact not only to future research and projects but also makes scientists and engineers reconsider their previous ideas in order to expand the tree of knowledge and technology that the humanity relies on.

1.3 Structure of the work

The presented Master thesis is divided into 5 chapters. Chapter 2 gives the necessary background about VECSEL, its concept, principle of working, design, as well as advantages. Chapter 3 describes the interferometric design of the laser external cavity. The chapter shows the evolution and different designs of the laser cavities based on interferometry. Moreover Chapter 3 explains the particular interferometric laser cavity and describes its peculiarities. Chapter 4 contains detailed descriptions of the real experimental setup, including all practical issues. Chapter 5 deals with experimental results obtained during the experimental work, and further discussions of results are placed. Conclusions about the done experimental work and future work discussion built the last chapter.

Chapter 2

VECSEL

2.1 Introduction

Throughout the history of lasers, lasers have been categorized according to characteristics such as an amplifying medium, output power, wavelength tunability, method of excitation, beam quality, device size and so on. Selection of the most important parameters for a particular application defines the type of laser.

Carbon-dioxide laser is the oldest gas laser and most powerful among other available ones. [12] It is widely applied mostly in industrial and medical fields; however, its wavelength emission is limited which, does not allow it to be used more actively. *Semiconductor diode laser*, on the other hand, by means of material selection, allows to obtain emitted light in rather big wavelength range from UV up to mid-IR, but output will be restricted by certain power limit.

Ti:Sapphire is a *solid-state* tunable laser which emits light in a quite broad range, from 650 to 1100 nm. Ti:Sapphire laser is capable of working in mode-locked regime due to its ability to emit very short pulses, but at the same time Ti:Sapphire demands optical pumping at the specific wavelength of 514 to 532 nm, which makes it less attractive [13].

Free-electron laser (FEL) it must be mentioned because this laser has the biggest range of the emitted light. Moreover, free-electron laser covers the part of light spectrum which is not attainable for other laser families – from X-rays to microwaves, which basically makes it very universal and peculiar. The widest frequency range and high output power of the laser open numerous perspectives for FEL, but a complex principle of operation involves expensive equipment and maintenance for the light generation [14].

Thus, before the introducing the optically-pumped VECSEL or OPSL (*optically-pumped semiconductor laser*) in 1997 by Kuznetsov [15] there hardly was a laser that could be ranked as a unique one, combining the advantageous properties and balancing the disadvantages of other lasers. In such a way, the development and further improvement of VECSEL gave an opportunity to overcome key problems related to disadvantages of pre-

VECSEL semiconductor laser era, such as achieving watt-level output power and maintaining satisfactory optical beam quality.

2.2 VECSEL as part of semiconductor laser family

VECSELs belong to the semiconductor laser family. Semiconductor lasers at the first order can be categorized by the their architecture.

Most semiconductor lasers are electrically pumped edge-emitting laser diodes which can be fairly named the most common and widespread lasers in the world. The edge-emitting architecture has a resonator, consisting of the gain media cleaved from one end. The dimensions of the gain media typically lie in the range between a few micrometers up to several millimeters, as shown on Fig. 2.1 (a). Electrical pumping of edge-emitting lasers allows modulating an output optical signal which, in its turn, makes the electrically pumped diodes very suitable for optical data transmission application. Edge-emitting lasers suffer from poor beam quality due to strong divergence of the light from very thin emitter structure.

Opposite to an edge-emitting architecture, a surface-emitting architecture exist, differences between which can be easily tracked from Fig. 2.1. Surface-emitting lasers are the newest subtype among the semiconductor laser's family [16]. Surface-emitting lasers further can be subcategorized into two groups: VCSELs (vertical-cavity surface-emitting laser) and VECSELs. Regardless the similar abbreviations the two above-mentioned categories are considerably different in their designs, characteristics and applications.

The crucial point in understanding the difference between both subdivisions can be easily perceived by the presence of the letter E in the abbreviation of VECSEL, where E – stands for external (cavity). Thus, VCSEL is a monolithic and compact laser device where the laser resonator has form of internal cavity implemented by two semiconductor Bragg mirrors and quantum well region sandwiched in between. The second significant distinction is that VCSEL usually are electrically pumped in comparison to mostly electrically pumped VECSEL.

Optically-pumped VECSELs consist of an external optical cavity made from semiconductor gain material with an integrated highly reflective semiconductor mirror or DBR (distributed Bragg reflector) and one or more external mirrors. One external mirror is supposed to be partially transparent in order to be used as an output coupler. The

configuration and geometry of the optical cavity are defined by the final purpose of the laser.

The OPS VECSEL allows to scale up the output power maintaining the circular output beam with the diameter of tens or even hundreds of microns, which can be possible only in case external cavity. Since VCSELs and laser diodes have a beam the diameter of which is limited by the thickness of the semiconductor chip, thus output power is limited. External cavity of the VECSELs provides a good transverse mode control that leads to excellent beam quality. By means of external optical elements, laser mode area can be easily increased under high pump powers in order to avoid thermal roll-over.

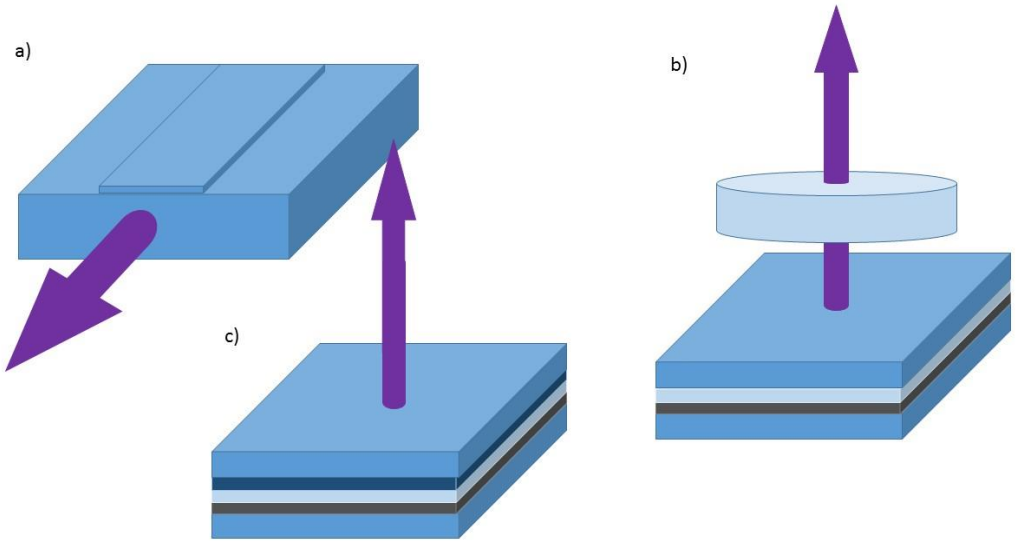

Figure 2.1: Schematic illustrations of: (a) semiconductor edge-emitting laser; b) semiconductor vertical-external-cavity surface-emitting laser with output coupler; c) vertical-cavity surface-emitting laser.

The presence of the external cavity as an integral part of the VECSEL increases the overall size of the laser and demands setting and aligning the cavity. But at the same time it allows inserting various intracavity components: nonlinear optical crystals for SHG (second-harmonic generation); optical filters, such as Fabry-Perot etalon for the selection of laser wavelength; saturable absorbers (SESAMs) for passive mode-locking. Second-harmonic generation is attractable technique for the generation of the visible light, since most of the VECSEL's semiconductor structures emit light in the infrared spectrum. Thus,

SHG twice expands the covered wavelength range. SHG utilizes the non-linear optical principle of two-photon absorption and allows doubling the output frequency of the light. Another fruitful application, which becomes possible due to external cavity, is a passive mode-locking. This laser regime can be achieved with the help of by SESAM, which is inserted inside the cavity as a cavity mirror. Mode-locked regime assumes the presence of ultrashort pulses train. Pulse duration can reach femtoseconds [17]. Combining multiple gain elements in series is also possible for obtaining higher-power laser operation modes [18]. Fig. 2.1 demonstrates the examples of VECSEL's external cavities.

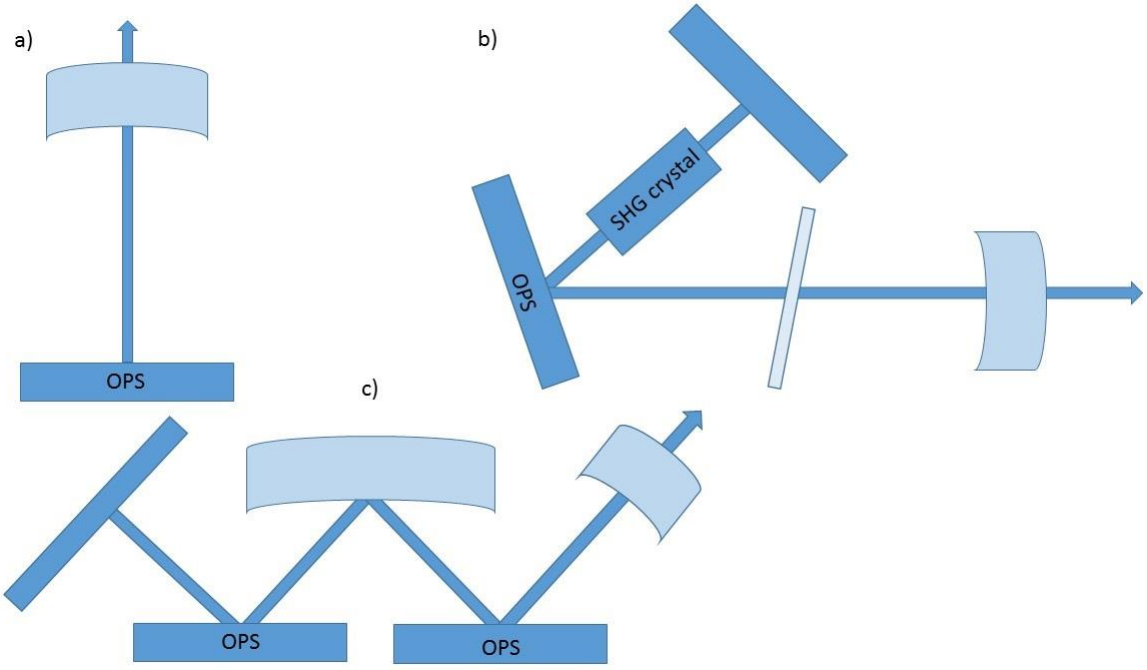

Figure 2.2: OP-VECSEL laser cavities. a) Linear cavity. b) V-shaped cavity for SHG with a Fabry-Perot etalon. c) Cavity with two gain chips [4].

2.3 Advantages of VECSEL

In order to summarize the general information about the VECSELs, it can be useful to sum up all the above-mentioned advantages of this laser family and show the applications of the optically-pumped vertical external-cavity surface-emitting lasers. The advantages are as follows:

- Wavelength scalability by means of gain material selection;
- Power scalability;
- Multi-watt output power levels;
- Excellent beam quality under the conditions of proper alignment of external cavity and pump mode matching;
- Fast semiconductor medium allows relatively low intensity noise to be achieved.
- Possibility of manufacturing the gain material as a wafer, which decreases it costs;
- Unnecessity of material doping;
- Optical pumping due to its tolerance to pumping light wavelength and possibility of using several pumps simultaneously;
- Presence of an external cavity allows inserting numerous optical components for different purposes.

VECSELs have vast applications at the consumer market. VECSELs are used in such fields as life sciences, for driving the fluorescent dyes at different wavelengths. VECSELs are on a great demand in medical therapeutics. Owning to wide wavelength tuning specific light frequencies can be obtained. Specific light frequencies possess the ability to interact differently with human body tissues. For instance, infrared light with a certain wavelength is used to activate drugs inside tissues due to good penetration depth of the incoming light. Dermatology and eye surgery remain important and common spheres of application for optically-pumped semiconductor lasers. VECSELs are the light sources which can be used in displays, because of high interest of suitable green light source, which can be provided by second-harmonic generation [19].

2.4 Operation principle and structure of VECSEL

Semiconductor lasers share the same main principle of operation nevertheless of numerous subdivisions inside the laser family. Selected semiconductor material such as GaAs, AlGaAs, InGaAs, InP etc., serve as an optical gain media, where stimulated emission occurs by means of interband transition, under the condition of high carrier concentration in the conduction band. Pumping of gain media leads to excitation of electrons and increasing number of carriers in higher states of conduction band, although carriers decays

rapidly to lowest states near the bottom of conduction band. Recombination of these electrons with holes at the valence band leads to photon emission stimulated by photons with the same energy and characteristics. Width of the interband transition is defined by semiconductor material selection, and as a result, material defines the frequency of emitted photons [20].

Basic structure of an ordinary VECSEL is composed from semiconductor chip consisting both of a distributed Bragg reflector and of a gain region (Fig. 2.3). The periodic structure of the gain region allows incident pump photons with higher energies to be absorbed in separate pump-absorbing layers. That leads to the excitation of carriers: electrons and holes, which further diffuse into quantum well regions with smaller bandgap energy, which in its turn leads to population inversion and as result make it possible further stimulated emission process. Achieving the proper material composition and layer thickness of the QW allows setting for the desired wavelength. QW were placed in the antinodes of the optical field [21]. Such a structure is called resonant periodic gain (RPG). RPG's length provides additional frequency selectivity for the operation wavelength. RPG's parameters are designed so that its length, under the pumping, will match the desired wavelength. The balance of pump-absorbing layers and quantum well regions sets lasers properties for the gain. Figure 2.4 illustrates schematically gain region structure.

A distributed Bragg reflector acts as a highly-reflective mirror for particular wavelength emitted by the structure of the gain. The DBR reflects photons allowing them to make a round trip across the cavity causing stimulated emission in the gain area. Nevertheless, pump light absorption reaches high efficiency inside the gain region even under thickness of 1 micrometer; efficiency can be further improved by placing a pump-reflecting mirror to obtain more round-trips for pump light inside the gain.

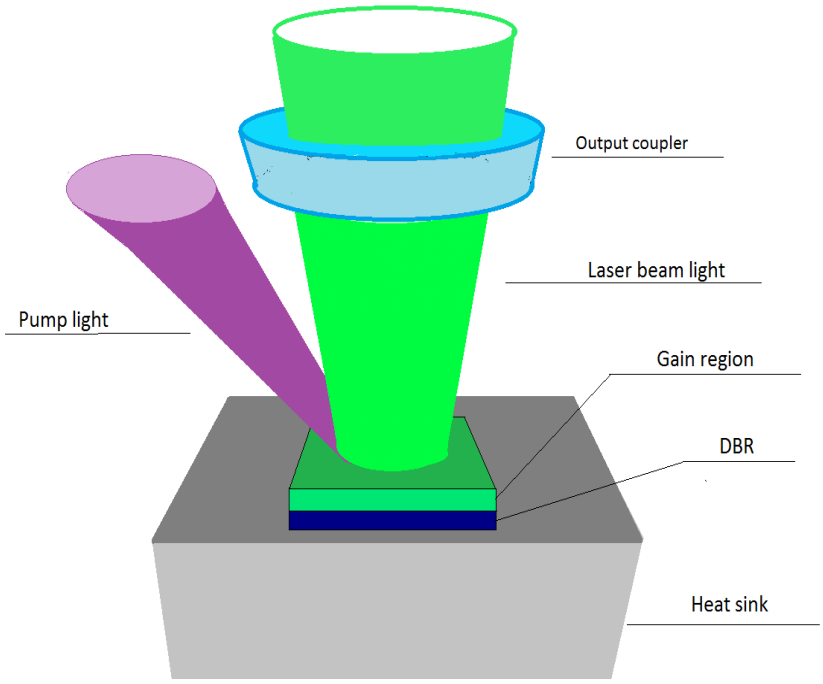

Figure 2.3: Schematic illustration of a VECSEL structure with the presence of external cavity. To simplify the drawing, the dimensions of the pump beam spot and output beam spot are not equal, even though they are supposed to be matched with each other in a properly designed cavity.

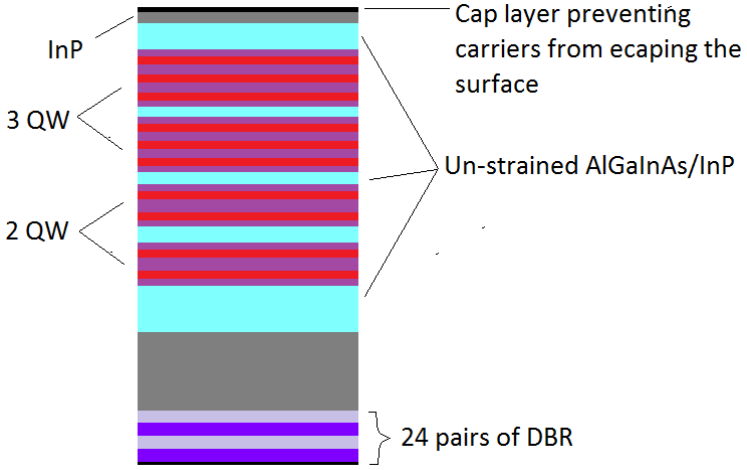

Figure 2.4: Schematic of the VECSEL gain structure

2.5 Optical pumping

The optical pumping of semiconductor lasers has a set of advantages over electrical pumping. The optical pumping of the gain region is implemented by means of a commercial multimode diode laser with the wavelength shorter than of the output beam. However, the pumping wavelength range can be rather wide and no custom require a particular semiconductor structure, which singularly simplifies the laser system. The optically-pumped semiconductor disk lasers have high tolerance for the pump's light characteristics. Thus, laser diodes with poor beam quality parameter can be used because of considerably small absorbing depths of the structure. Comparing the OP VECSELs to most solid-state lasers, it must be said that solid-state lasers can withstand neither poor values of the pumping beam quality, nor a wide range of pumping wavelength [22].

By means of optical pumping and by controlling the external cavity elements, carrier excitation is possible across a considerably wide area ranging from 50 to 1000 μm, which allows scaling up the output power to higher values without consequent thermal damage. Theoretically, there is no restriction to the number of optical pumps supplying the gain region. Therefore, several lower power optical pumps can be used instead of one highly-powered one. That fact makes optical pumping more practical and affordable.

2.6 Thermal management

Some VECSEL's parameters are temperature dependent, for example, output spectrum, distribution of electron states, bandgap. An increase in temperature decreases the bandgap, which leads to shifting QW spectrum towards longer wavelengths at the rate of ~ 0.3–0.5 nm/K, while the optical length of resonant periodic gain (RPG) shifts at rate ~ 0.1–0.2 nm/K [23,24]. In such a way, the QW wavelength can no longer coincide with the RPG resonant wavelength, which leads to limiting the output power at some pump power levels (Figure 2.5). Moreover, because of thermal expansion and presence of temperature gradient inside the gain material or heat spreader, if included, the thermal lensing effect can be observed. Thermal lensing changes the physical and optical path of the external cavity and as a result leads to decreasing of beam quality. Thus, thermal lensing changing the original cavity design with increasing of pump power.

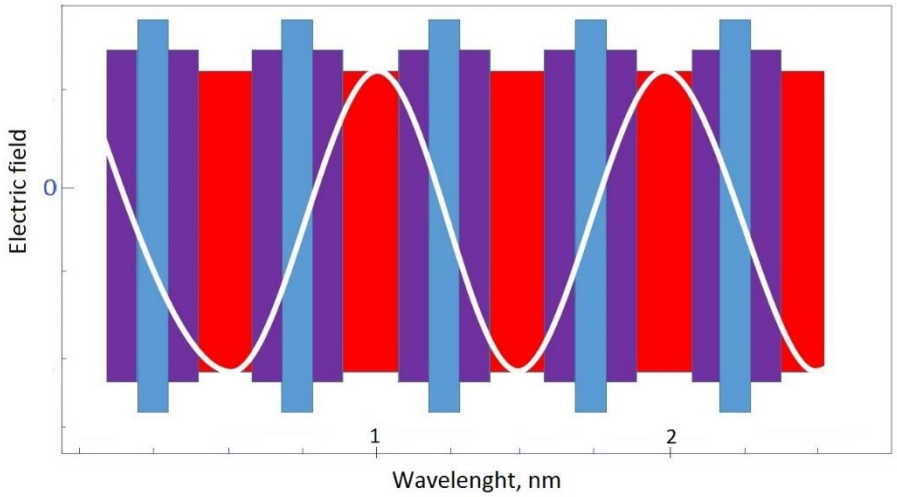

Figure 2.5: RPG structure. Resonant wavelength (white) matches with resonant periodic gain structure consisting of QW (purple and red regions) and un-strained regions (blue).

The photon energy difference between the incident pump light and the emitted one causes a quantum defect that can be named as one of the main contributor to the laser losses resulting as a heat [25]. Moreover increasing the pump power leads to rise of the chip temperature and as a result raised temperature leads to an increased amount of non-radiative recombinations [26]. In order to efficiently dissipate heat excess from the device active region heat spreaders are widely used. Heat spreader connected to the heat sink can be placed on the bottom of the semiconductor chip, or it can be a transparent heat spreader, such as a natural diamond mounted on top of the semiconductor surface. In case of the transparent intracavity diamond the heat spreader should be AR coated for better laser performance.

Thus, VECSELs can be subcategorized due to the absence or presence of heat spreaders on top of the semiconductor surface. These VECSEL categories can be named, for further bordering, as flip-chips and intracavity diamond chips Fig. 2.6, 2.7.

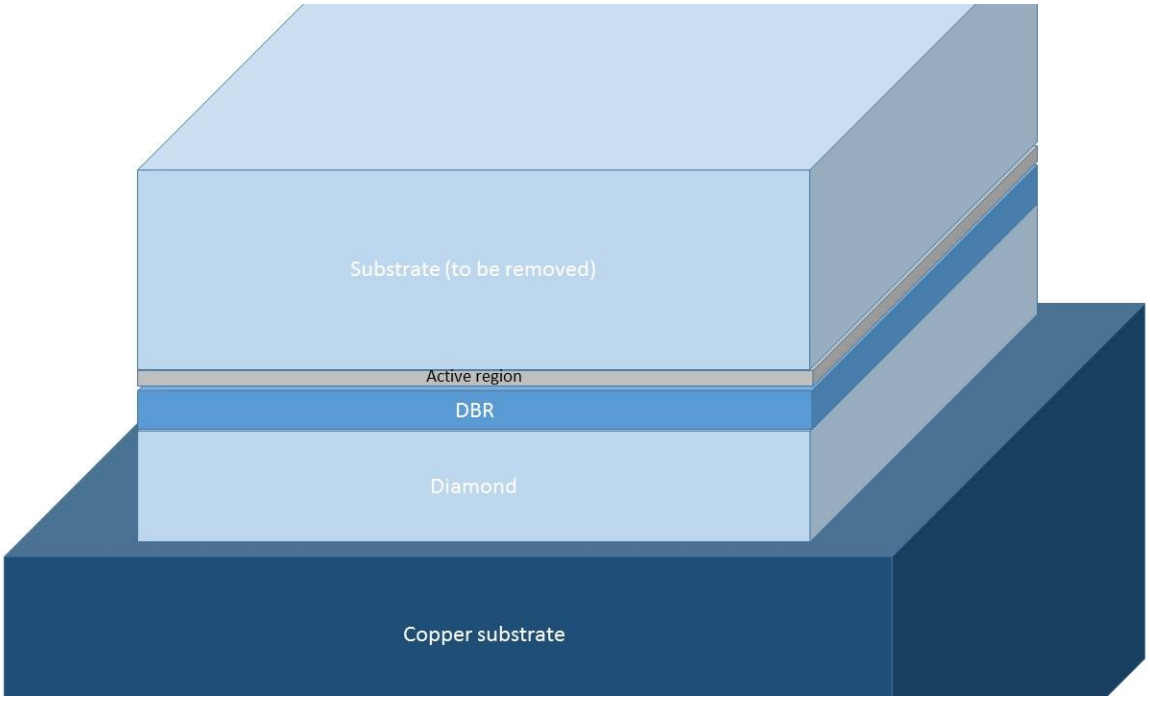

Figure 2.6: Flip-chip structure.

The flip-chip configuration assumes the mounting VECSEL structure onto diamond heat-sink, usually using borderline metal layer. After removing a substrate from the top of the structure, VECSEL-diamond assembly placed onto copper plate, for instance, by means of indium soldering. Further copper plate is supposed to be cooled by any means, like water-cooling or TEC, depending on the purpose. The excess of heat during the operation flows through DBR section. Therefore, thermal properties, such as thermal conductivity and thermal resistance of semiconductor components, which are used in particular DBR, should be taken into account. In such a way designing and material selection of DBR play a significant role in flip-chip configuration.

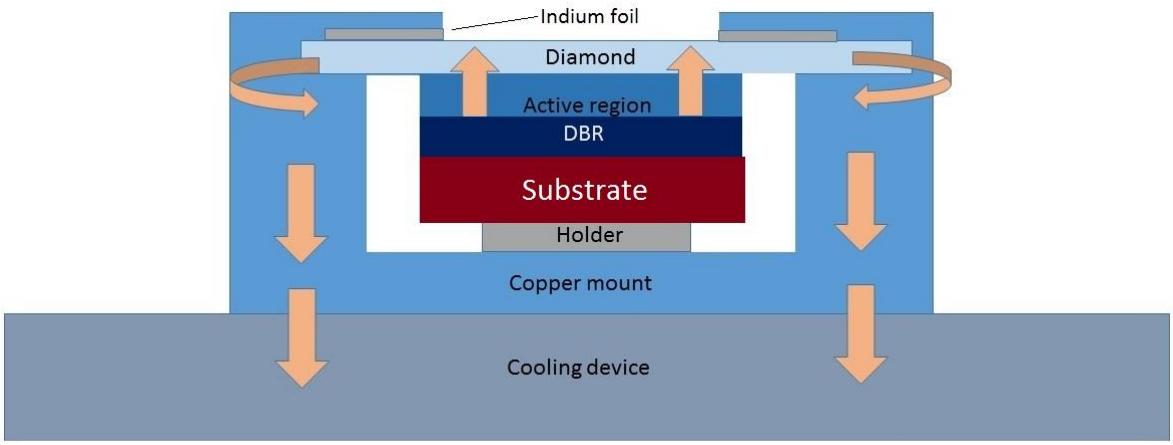

Figure 2.7: Cross-section of intracavity diamond chip mount. Heat flows are marked by arrows.

Intracavity heat spreader is bonded to semiconductor structure capillary by means of distill water or alcohol [27]. Vander der Waals forces pull the surfaces in close contact. Bonding remains stable by applying constant pressure with a copper holder. Intracavity heat spreader approach simplifies heat extraction from a gain region but at the same time, it brings negative effects such as modulating output signal, because intracavity diamond works as a Fabry-Perrot etalon. In this work chips with intracavity heatspreaders have been used. Because of etalon effect intracavity chips (IC) provide, the flip-chip configuration happened to be more attractive. It will be explained in details in experimental part section.

2.7 VECSELs in this work

Four VECSEL chips have been used in this Master's thesis work. The wafer-fused chips share the same design of the gain structure. However, they come from different batches of semiconductor growth. Particular semiconductor chips presented in this work have InP-based 3-3-2-2 QW structure. The 6.7 nm thick AlGaInAs QW were sandwiched in between 10 nm AlGaInAs strain compensation layers absorbing the pump light. Working wavelength of the laser is 1.27 μm chosen to potentially obtain red light by means of SHG. A photo of one of the VECSEL chip is shown in Fig. 2.8:

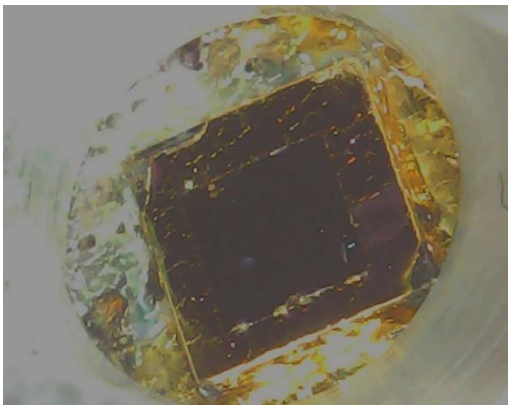

Figure 2.8: Photo of one of the 1.27 μm VECSEL flip-chips used in the experimental setup. The chip's dimensions are approximately 2x2 mm. The surface of the sub-mount is covered by a gold layer for bonding purposes and better heat extraction from the chip.

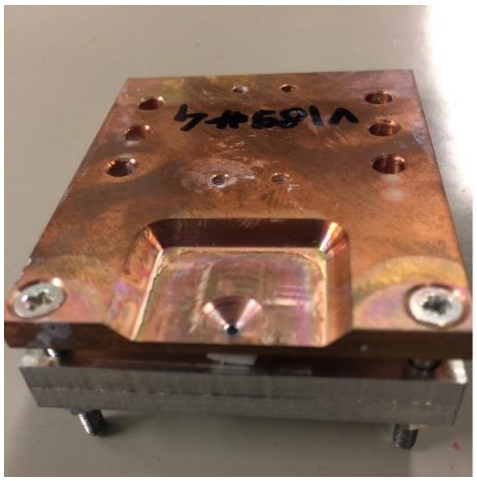

Figure 2.9: Photo of the IC VECSEL chip mounted in copper holder (Fig. 2.7).
The diameter of the aperture in the holder is 1.5 mm

Chapter 3

Interferometric lasers

3.1 Introduction

Interferometers are scientific devices, which are highly demanded in numerous fields of engineering and science, such as astronomy, metrology, fiber optics, spectroscopy, quantum mechanics, nuclear and particle physics, remote sensing [28]. There are many types of interferometers, although all of them share the main principle of working based on interference between waves. Interference is a physical phenomenon, which occurs between superimposed waves. Interference can be observed in all types of waves: light waves, acoustic waves, mechanical waves; although in most cases under term of interference is common to understand interaction between electromagnetic waves. Interference happens between two or more waves under the set of condition: they are supposed to be coherent and correlated and must have nearly the same frequency. The optical intensity of the resultant wave equals to the vector sum of the optical intensity amplitudes of the interacting waves. Constructive or destructive interference can occur depending on the phases of the waves. Interference between the waves can leads to either mutual canceling or creating a resultant wave, which will be, amplified (Fig. 3.1)

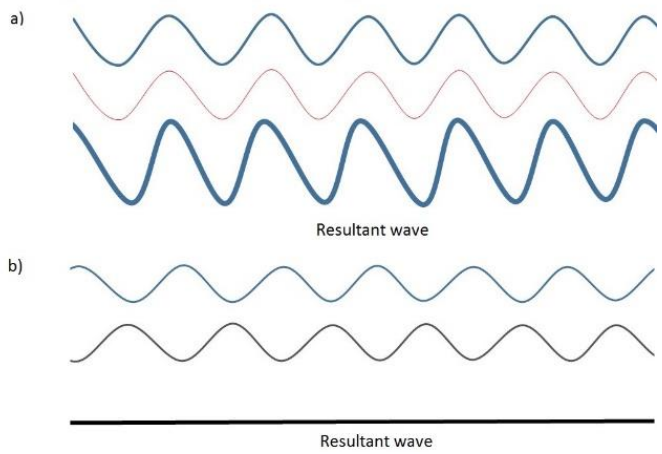

Figure 3.1: Resultant waves after the interaction of two waves, which have: a) the same phases; b) opposite phases.

Diffraction and interference can be perceived as the matter of the same phenomena. Scientific community has not bordered these two concepts very strictly, so these terms can be mutually replaced, although, term "interference" commonly refers to wave interaction of two wave sources, whether term "diffraction" refers to uncountable interacting sources [29]. Interference can be spotted in everyday life, one of the most common example of interference occurs in thin films, for instance soap bubble or thin layer of gasoline. In this case, interference happens between reflected waves from the front surface and back surface of the thin film. Resulting constructive or destructive interference depends on the thickness of the film, therefore varying thickness in a film leads to appearance of colorful reflection.

Interferometers exploit the meaningful information that the resultant wave gives about the properties of the combined waves. On one hand, interference can be applied in order to transform two waves incoming from different sources, for instance, to combine them and amplify. On the other hand, other interferometric designs can use only one incoming beam, which further will be split by a beam splitter (BS). After that, taking into account the purpose of the interferometric design, investigation of these two beam's interference is conducted.

3.2 Interferometry

Interferometry can be described as a set of techniques that utilize the principle of interference. Interferometry is an extremely ubiquity investigative technique. It has found a countless number of applications in science and technology. Apparently, the first well-known experiment involving the interference and interferometer, which led to the giant breakthrough in the reconsidering the laws of Physics, was Thomas Young's double slit interferometer experiment, conducted at 1803 [30]. The experiment became a foundation on which the wave theory of light has been built. After the invention of quantum mechanics this experiment was given a new life, serving as an example of wave-particle duality demonstration. Famous physicist R. Feynman used to say that careful thinking about this experiment can leads to full implication of quantum mechanics theory and its laws, only from one experiment [31].

Interferometric setups, which have been described further, generalize the idea of interferometry applied to many fields, independent on light used in it. Obviously, the first interferometers utilized a white light, mostly, before the invention of the first masers and then lasers. White light has considerably low coherence length compared to the laser light, which in practice makes obtaining interference difficult.

Coherence length of the light is one of the most important characteristics in interferometry. Coherence length equal to the propagation length after which phase shift between the waves will be equal to π. Coherence length arises from the white noise of the source and depends on a linewidth of the source output spectrum. For the sufficient level of interference, coherent length of the light source, which used in the particular interferometer, should exceeds the interferometer optical path. There are a lot of different available light sources, the coherence lengths of which differ drastically. The coherence length may be described by the equation [32]:

$$l = \frac{c}{n\Delta\omega} \ , \tag{3.3}$$

where c is a speed of light, n represents refractive index of a medium, $\Delta\omega$ corresponds to source bandwidth. In such a way, the one can perform a calculation in order to obtain the coherence length of a white light. Assuming that border of visible light starts at $\omega_1 = 4 * 10^{14}\ Hz$ and ends at $\omega_2 = 7 * 10^{14}\ Hz$, the coherence length equals 0.5 μm, when the

coherence lengths of semiconductor lasers usually reach orders of hundreds of meters. An obvious conclusion about the benefit of utilizing lasers in interferometry can be made.

One can categorize interferometers by variety criteria. For instance, homodyne and heterodyne detection techniques may be distinguished in interferometric techniques . In homodyne detection, interference happens between waves which have the same, or nearly the same frequency. In such a way, interference between waves with the same wavelength leads to changes in output intensity of the combined beam. The magnitude of intensity and interference patterns, further to be measured, recorded and processed, become an outcome of homodyne detection subdivision. Homodyne detection is used in the most of interferometers, such as well-known Michelson interferometer. Homodyne interferometer has been presented in this work.

3.2.1 Types of interferometers

The path of the light may further categorize interferometers: there can be either common path interferometers, such as Sagnac interferometer (Fig. 3.2), or double path interferometers, such as Mach-Zehnder (Fig. 3.3).

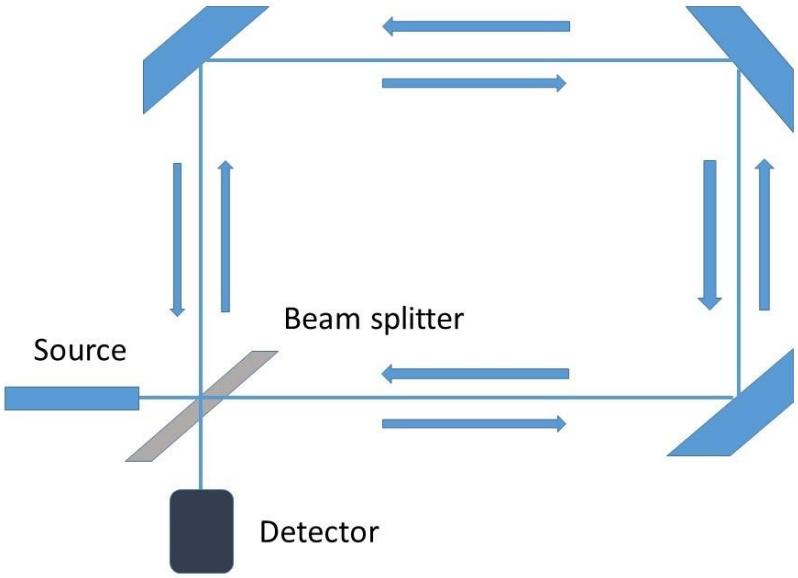

Figure 3.2: Sagnac interferometer. Arrows show light paths.

Fabry-Perot interferometer is perhaps the most widespread and simplest interferometer (Fig. 3.4). Fabry-Perot interferometer consists of two highly reflective mirrors, one of which has somewhat smaller transmittivity than the other one. In principle, Fabry-Perot interferometer works as a standing wave resonator, where light trapped inside the resonator experiences an interference, either destructive or constructive, dependent on wavelength and thickness of the resonator cavity. Such interferometer, for instance, can be placed into the external cavity of the laser and then provides frequency dependent transmission, which can be seen in the output spectrum of the laser (Fig. 3.4). In such a way, Fabry-Perot etalon inserted into the resonator cavity of the laser may favor one longitudinal mode over other modes in the laser gain bandwidth, and thereby enable single frequency operation.

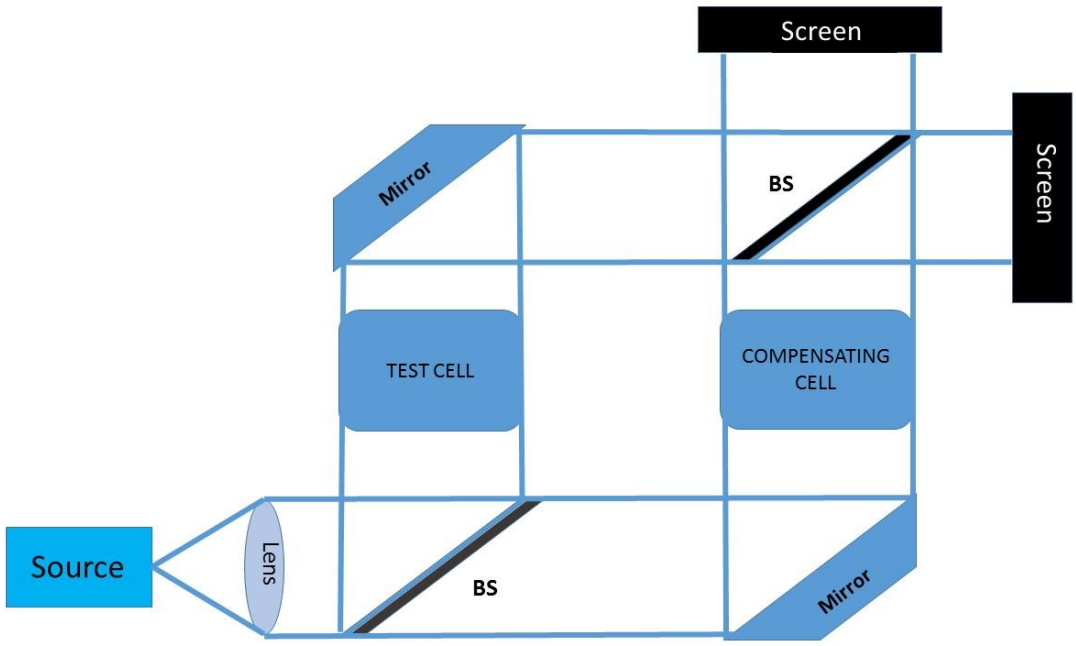

Figure 3.3: Mach-Zehnder interferometer.

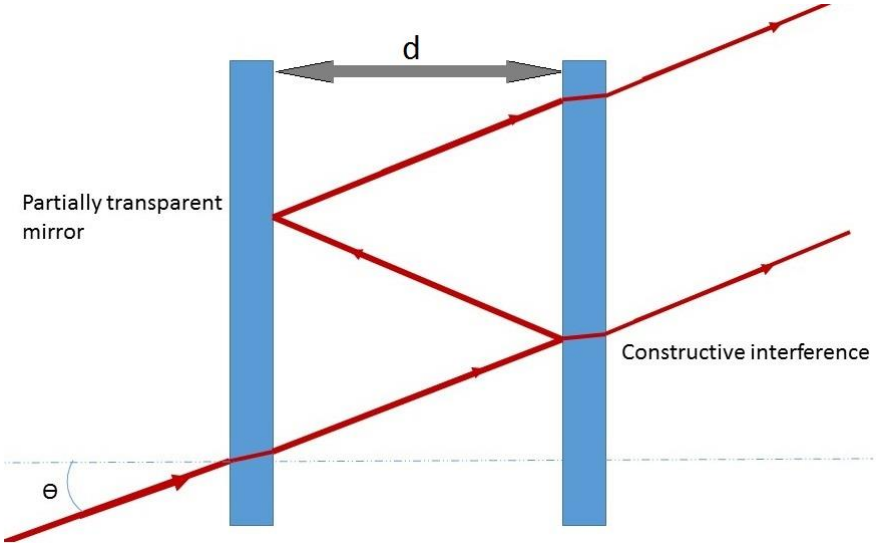

Figure 3.4: Fabry-Perot interferometer

Due to strong wavelength selectivity, Fabry-Perot interferometer also has found its application as a high-resolution spectrometer. These sharp peaks of transmission can be tuned by means of changing the distance between the mirrors using piezo actuator. Hence, applying voltage to the piezo and monitoring the transmitted optical power versus time can give as a result the optical spectrum of the incident light.

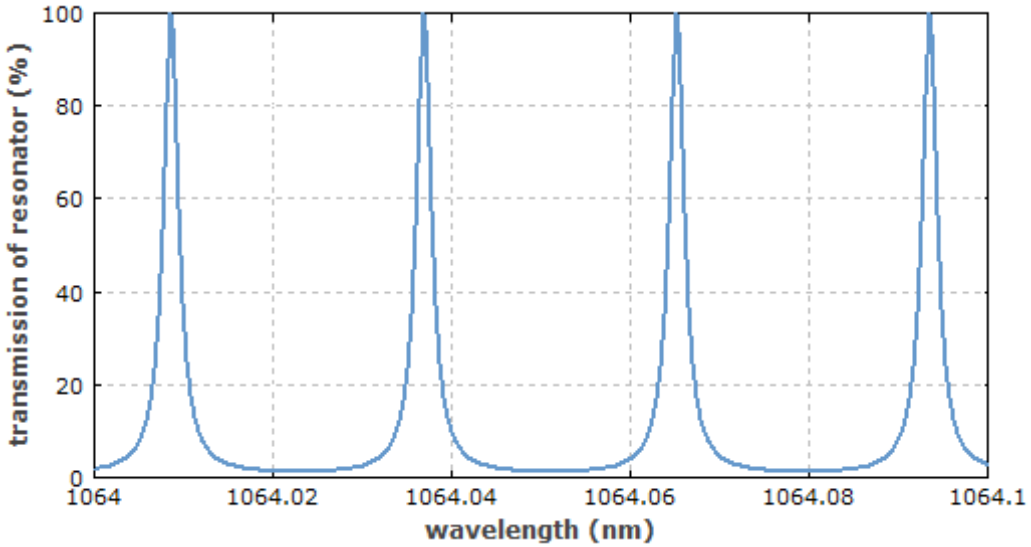

Figure 3.5: Fabry-Perot interferometer's frequency-dependent transmission. Mirror reflectivity equal to 90% [1].

Sagnac interferometer can serve as another interesting case of an interferometer design. The mentioned interferometer relies on Sagnac effect [33]. This particular interferometer would not achieve such popularity without lasers. Sagnac interferometer has been already mentioned in this work as an example of the common-path interferometers. For the simplicity of understanding, the Sagnac interferometer's principle of working is shown in Fig. 3.6.

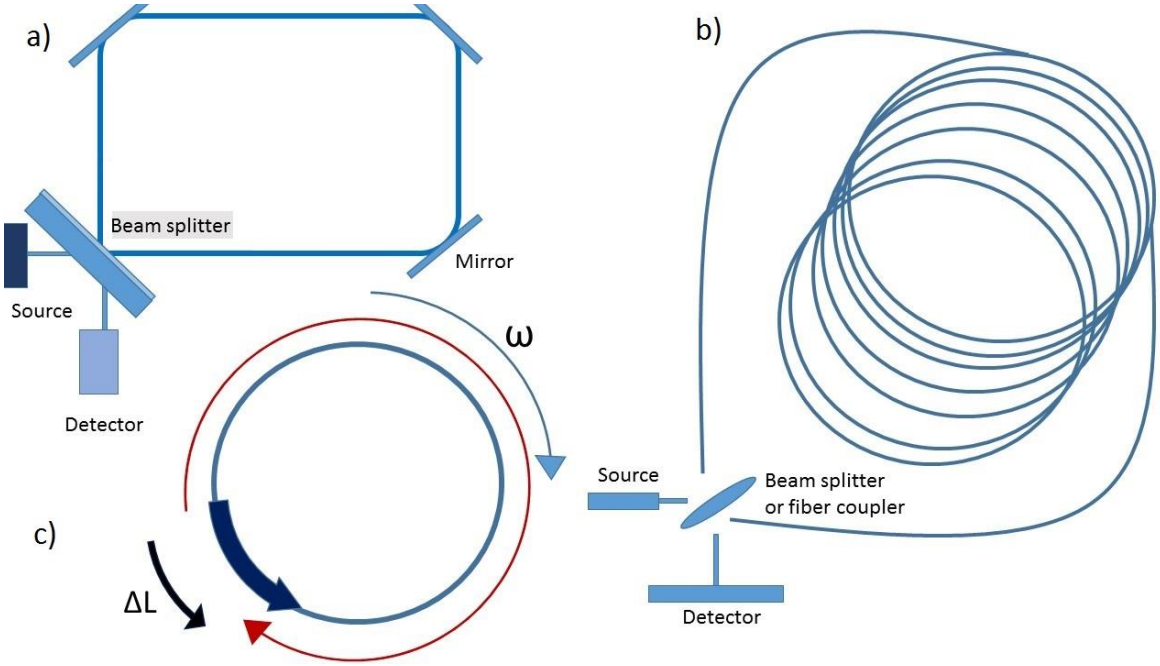

Figure 3.6: a) Sagnac interferometer. b) Fiber ring interferometer. c) Illustration of the phase difference in counter propagating beams.

Sagnac interferometer has been invented in attempt to prove the aethir theory, as well as Michelson interferometer [34]. Laser era made it possible to use the principle of Sagnac interferometer as an extremely precise laser gyroscope, shown in Fig 3.6 (b). The principle of operation can be understood as follows. One can imagine a moving mount with laser ring gyroscope on it. Laser source with a satisfactory coherence length produces a beam which is further divided into two beams. These beams further enter an optical fiber ring from opposite ends and counter propagate through the fiber. The rotational moving of the mount with the laser ring changes the distance which light should travel in each direction.

It should be noted that the rotation of the fiber ring does not change the speed of the light propagating inside the fiber, but rotation affects the *length* of the light path (ΔL) , so light needs less or more *time* to reach the same point, depending on the direction of propagation:

$$\Delta t = \frac{4\pi R^2 \omega}{c^2}, \tag{3.5}$$

where ω is an angular velocity, R is the radius of the fiber ring and c corresponds to the light speed. Therefore, rotation causes the waves to reach the beam splitter out of phase relative to each other. The long fiber ring makes it possible to achieve exceptional precision (after the analyzing the interference picture at the output).

The Michelson interferometer flipped over the outdated understandings about the laws of nature and significantly influenced the development of modern science. Furthermore, the Michelson interferometer serves as the basis for the experimental VECSEL setup presented in this thesis.

Operation principle of the Michelson interferometer can be understood from the Fig. 3.7. It consists of two HR mirrors designed for a particular wavelength, beam splitter, which splits the beam from the source into two beams and the detector. Beam splitter is a corner stone of the Michelson interferometer and it may be a half-silvered mirror, as it was in the original Michelson interferometer, either beam splitter can take form of dielectric mirror. Dielectric mirrors consist of many layers of materials with varying refractive indices designed so that at an angle of 45 degrees half of the light will be transmitted through the beam splitter and rest of the light will be reflected. Usually non-polarizing beam splitter are used.

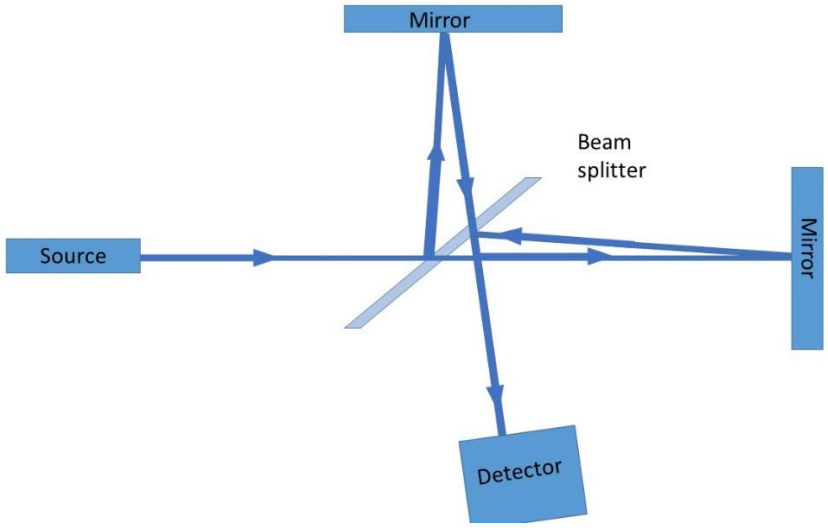

Figure 3.7: Schematic illustration of the Michelson interferometer

After the beam splitter the source light becomes divided into two beams which travel two different paths, recombine at the splitter and reach the detector. Varying the distances of the interferometric arms changes the phase of the recombining rays, and therefore leads to alteration of the splitting ratio between light directed to the detector and light directed back towards the source. Hence, Michelson interferometer can be a useful instrument for precise measurement of the physical path lengths, or for measuring the refractive index of the path.

Michelson interferometer is the best known from the famous Michelson-Morley experiment conducted in 1877 by A. Michelson and E. Morley [35]. The experiment is considered as the most important one in the history of humanity which yielded negative result. The main idea of the experiment was linked to the attempt to detect the relative motion of so-called liminiferous aethir. Concept of the liminiferous aethir claims there is a medium, called “aethir”, which works as light-bearing medium, through which light can propagate. Earth motion through the aethir was supposed to cause the “aethir wind”, which in theory was expected to cause the changes in the light speed, whether increasing or decreasing the total velocity of the electromagnetic wave, depending on a direction of propagation. Thus, the Michelson interferometer has been built in order to detect the difference of the time which light rays demand to travel through different paths. In aethir theory, the light was expected to behave as it shown at the Fig. 3.8 by dashed lines.

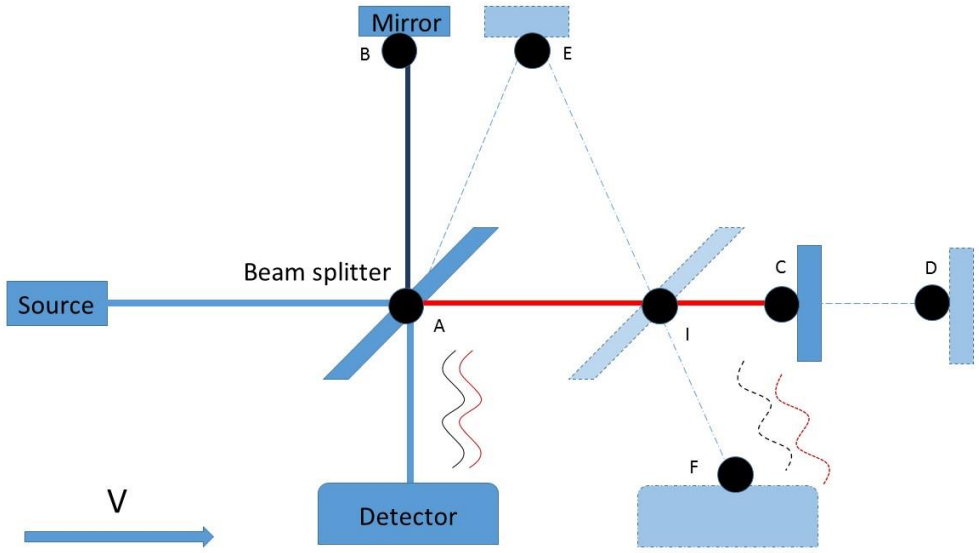

Figure 3.8: Schematic setup of Michelson-Morley experiment. By an arrow Earth's motion is shown. Dashed lines show predicted light paths. Light paths AB and AC are taken as ones having identical optical length.

Taking into account the different time needed to complete these two different paths, it was fair to assume that the two waves would be recombined with different phases, and therefore corresponding interference pattern was expected. Although the whole experiment was proved wrong. Thus, the time spent passing two different paths were equal, a fact of which led to upper limit of the light speed. Hence, Michelson-Morley experiment that yielded null-results became a foundation for further formulating of the special relativity theory by Einstein in 1905 [36]. The failed experiment brought the biggest benefit for further researches.

As it was mentioned above, interferometers play a crucial role in spectrometry. Michelson interferometer is widely used for obtaining digital spectrum of light, as well as previously mentioned Fabry-Perot interferometer. The spectrum of light has a major influence on the interferogram observed during changing of the optical length of an arm of an interferometer. Spectrometry utilizing the Fourier transform is a direct application of Wiener-Kinchine theorem [37]. An experimental setup for Fourier spectrometry exploiting Michelson interferometer can take a design as pictured in Fig. 3.9.

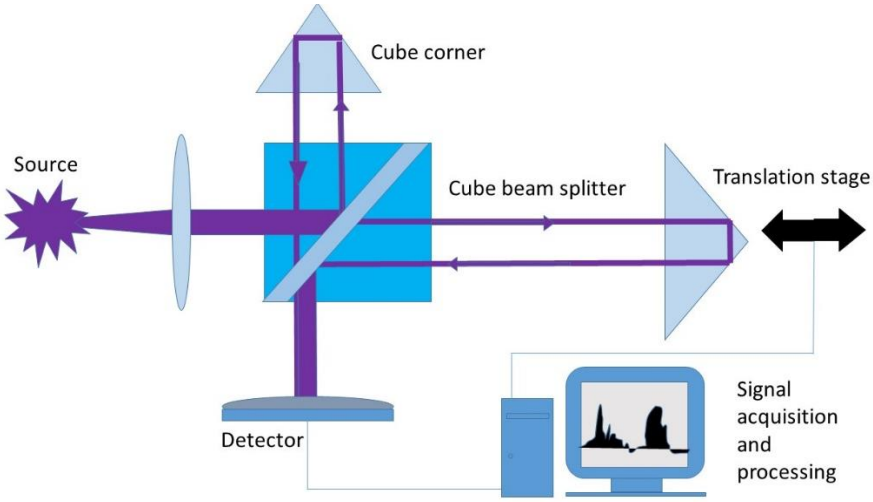

Figure 3.9: Fourier spectroscopy with a Michelson interferometer. Mirrors are replaced by cubic corners because it makes possible to change the length of one arm without ruining the initial alignment, as it can happen with setup pictured in Figure 3.5.

Despite the fact that interferometry usually associates mostly with electromagnetic waves, interferometry principle recently used in Laser Interferometer Gravitational-Wave Observatory (LIGO) project experimentally confirmed the existence of gravitational waves and their impact on matter [38,39]. Apparently, LIGO interferometers, which consist of Michelson and Fabry-Perot interferometers, can be granted the status of the biggest human-built interferometers. Their arms are 4 kilometers long. One may find irony in that Michelson interferometer first brought null results, which became the origins for the special relativity theory and after more than 100 years, observatories equipped with almost the same Michelson interferometers detected experimental evidence supporting general relativity theory.

3.3 Interferometric lasers

After the invention of laser it became clear that lasers had started to be an essential and irreplaceable part of the interferometry. What is even more interesting is that mutual benefit were achieved. In other words, lasers not only considerably affected the whole interferometry field, but in addition, lasers have been influenced by the interferometric principles that penetrated deeply into many laser designs and specific applications.

Interferometric laser designs can utilize the coherent beam combining technique, which scales up the output power without lowering beam quality. [40,41]. As it was showed by Ishaaya, two or more solid-state lasers can be interferometrically combined with total output power almost matching the sum of the power of the individual lasers. Such design has been pictured in Fig. 3.10.

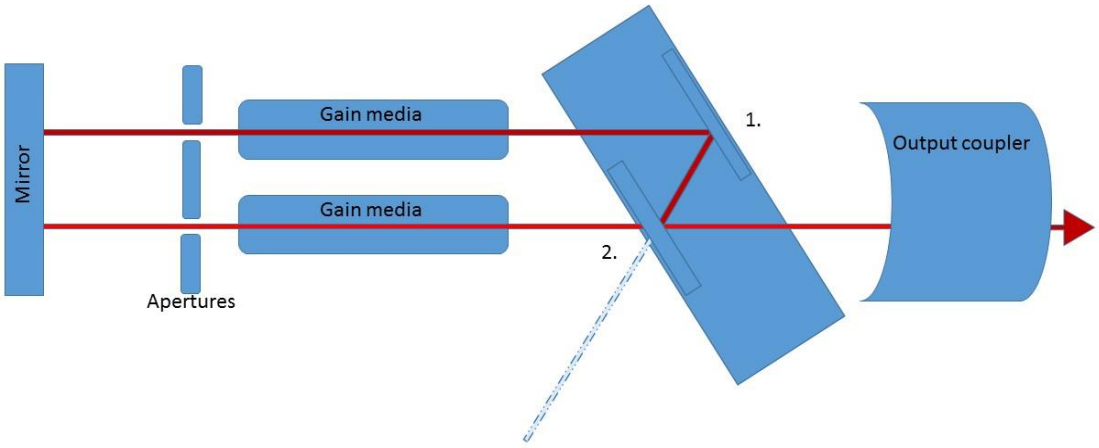

Figure 3.10: Laser design for intracavity interferometric combining. Solid-state gain media have been used. Point 1 depicts highly reflective coating, whereas point 2 marks 50% beam splitter coating, where interference takes place.

The thickness of the interferometric combiner and its angle relative to the incident beams allow the two beams to overlap optimally. Such a design can be performed with an array of solid-state rods and a set of combiners. Total combining efficiency can reach 90% [42].

The laser presented in this Master thesis also based on the principle of interference. The setup exploits interference as a strong and efficient method for frequency mode discrimination. The mode discrimination technique is used in order to receive narrowed output spectrum of light. It can be implemented by means of suppressing resonator modes at undesirable frequencies. Narrowing the spectrum can be performed by creating enough losses inside the cavity for unwanted frequencies. One can imagine a filter inside the

resonator, which will be almost entirely transparent for some wavelengths and will cause losses for other wavelengths. Some frequencies in the gain bandwidth will have negative gain factor, i.e. losses at these exact frequencies will be greater than the gain, whereas other frequencies will experience positive gain factor. In principle, frequency selection method does not mean negative changes in output power. Instead, photons of undesirable wavelength will be subsided, allowing other photons to create more photons of allowed frequency.

Practical usefulness of lasers that operate in the single-frequency regime can be explained by the almost ideal beam quality of such lasers, their huge coherence and the decreased level of noise in such devices. Hence, single-frequency lasers find a lot of applications in many, such as high-resolution spectroscopy, efficient nonlinear frequency conversion and optical fiber communications [43].

Stable single-frequency operational can be conventionally achieved with a distributed feedback lasers (DFB lasers), the whole resonator of which consists of a periodic structure that works as a DBR [44]. However, such laser diodes cannot produce high output power.

It is worth mentioning that any laser family, which includes an external cavity, becomes interesting due to the possibility of switching them into single-frequency regime. External cavity assumes the possibility of changing the parameters of it: angles and lengths. Therefore, a simplest external resonator cavity can be considered as Fabry-Perot interferometer with an adjustable length and beam path. Due to interference, both destructive and constructive inside the interferometer, Fabry-Perot resonator allows only discrete frequencies to create standing waves inside it. The discrete number of frequencies, which can match a Fabry-Perot resonator with a defined length, can be described by the equation.

$$N = \frac{2L}{c}\,\Delta\omega, \tag{3.6}$$

where L stands for resonator length, c for speed of light , and $\Delta\omega$ represents the gain bandwidth.

In such a way destructive interference that occur for some wavelengths contribute to the losses. Lasers happen to be extremely sensitive to any losses inside the resonator, thus losses equal to a couple of percent can lead to mode suppression at these frequencies in

favor of frequencies that experience the constructive interference. VECSEL's spectrum with intracavity diamond as a heat spreader, which serves as an example of frequency selectivity provided by the thin diamond, is shown in Fig. 3.11.

Michelson interferometer, in principle, can be considered as two Fabry-Perot interferometers combined in one resonator by means of beam splitter. Such configuration becomes a passive mode filtering technique, when combined with a light amplifying medium.

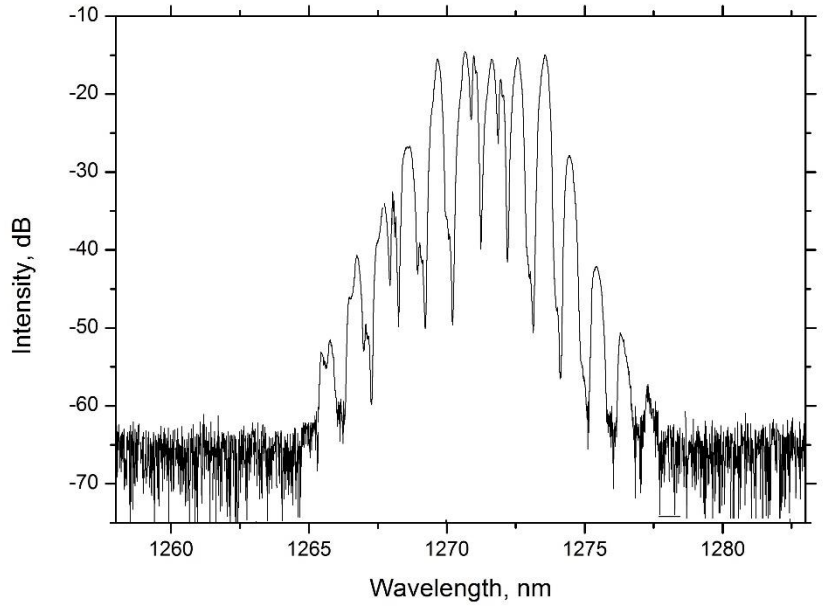

Figure 3.11: Output spectrum of VECSEL with a Fabry-Perot etalon inside the resonator cavity. Spectrum obtained by means of optical spectrum analyzer.

In 1966 DiDomenico presented a single-frequency laser with a Michelson interferometer in its core, which provided single-frequency output. [45]. The original setup was built using He-Ne gain medium with the operation wavelength of 632 nm. Fig. 3.12 shows the laser setup design.

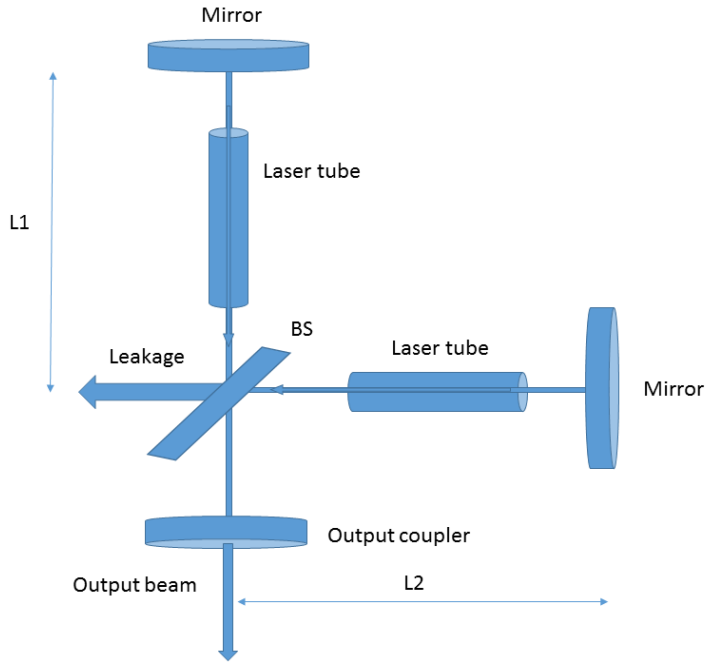

Figure 3.12: Interferometric design for the frequency selection.

The main idea can be understood as follows: Michelson interferometer with no difference in the length of two arms works as a regular Fabry –Perot interferometer. However, small difference in the optical path lengths leads to a considerably different final picture. It can be understood as an additional filtering effect provided by a beam splitter. The beam splitter, which will combine the waves from the arms with different length, will have a transmission loss per one-way pass that can be described by the equation [45]:

$$T_c = \frac{8sin^2(q\pi\Delta L/L)}{1+8sin^2(q\pi\Delta L/L)}, \tag{3.7}$$

where $q = 0, \pm1, \pm2, \dots, \pm L/\Delta L$ is the qualitative factor of the mode. ΔL represents the difference in the path lengths of the two arms. This transmission loss is independent on a beam splitter reflectivity.

The dependence of modes discrimination on ΔL and the quality of mode is presented schematically in Fig. 3.13:

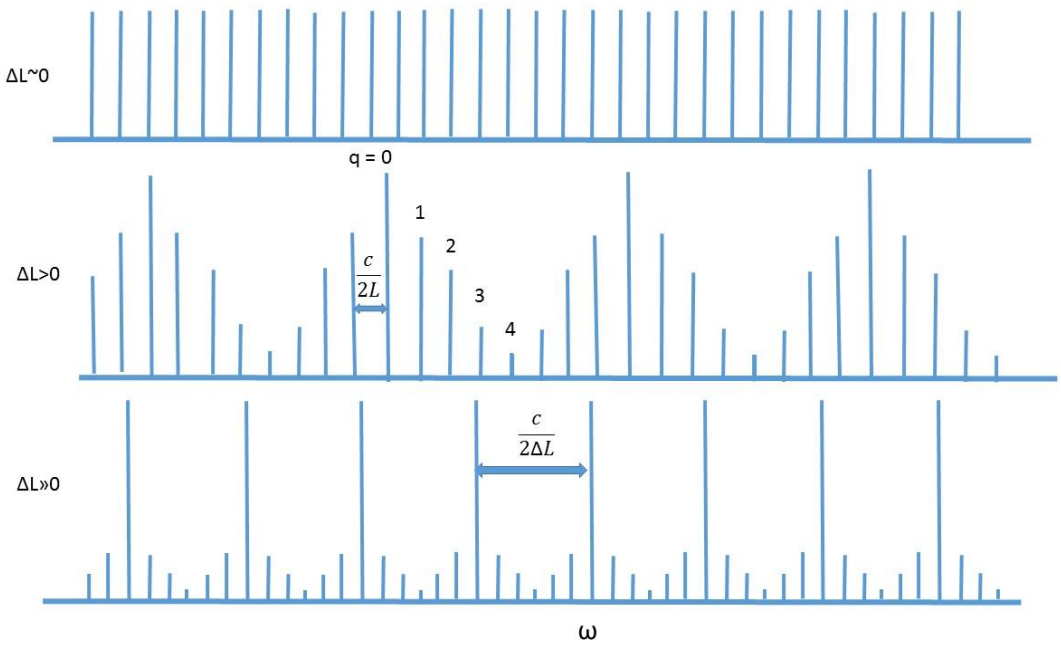

Figure 3.13: Frequency mode spectrum of Michelson-type laser. The vertical axis shows the intensity of the longitudinal modes of the laser, represented by blue vertical lines. Horizontal axis corresponds to the frequency of the modes. Parameter q, starting from 1, shows the qualitative degree of the mode suppression.

Length L defines the separation between all modes, similarly to Fabry-Perot interferometer. When ΔL is responsible for the rate of mode suppression and separation distance between q=0 modes. Therefore, single-frequency operation can be made possible under the condition:

$$\Delta L \leq \frac{c}{2\Delta\omega}, \tag{3.8}$$

Which ensures that only a single high-quality (q=0) mode lies frequency within laser bandwidth. Increasing ΔL brings the modes with q=0 closer. Increasing ΔL also leads to increasing of mode discrimination level against non-coincident frequencies (q>0). Therefore the frequency which falls within gain bandwidth is supposed to have gain exceeding the losses. Hence, ΔL parameter, chosen for successful single-frequency operation, is limited by these two border conditions: there is should be only one coincident

frequency within the gain bandwidth and all other modes should be efficiently suppressed, in order to prevent them from lasing.

The work presented in this Master thesis is the first experimental attempt to combine two VECSELs into one interferometric design with the final aim of scaling up the output power of the laser and obtaining single-frequency operational regime.

Chapter 4

Experimental laser setup

4.1 General overview

The experimental part of this M.Sc. thesis included building a multichip interferometric VECSEL. The basic design of the setup is shown in Fig. 4.1.

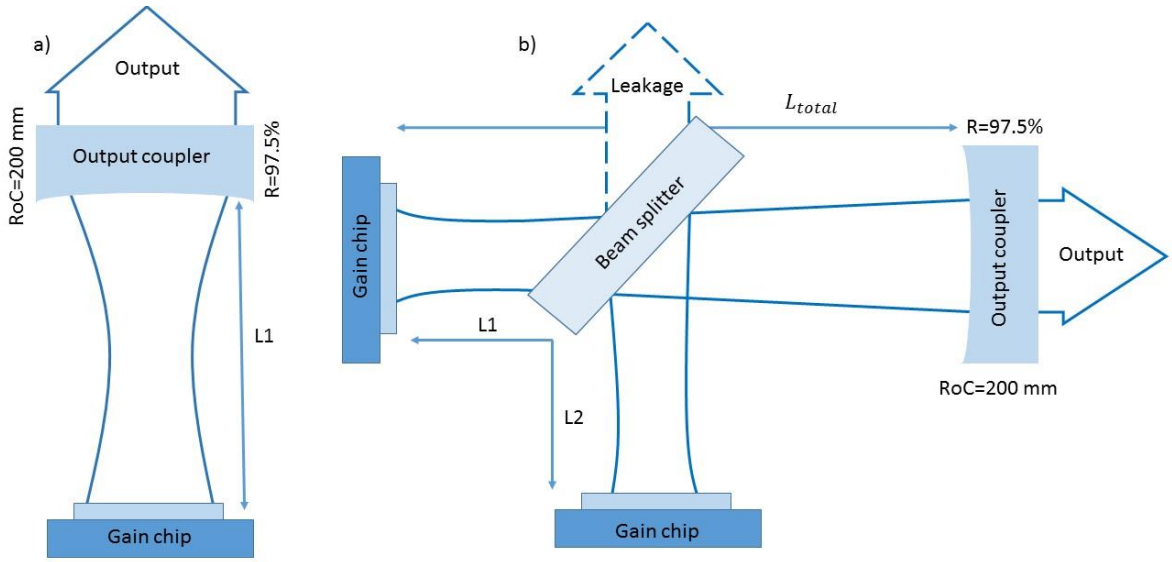

Figure 4.1: Laser setup design of: a) linear single-chip cavity; b) linear multi-chip cavity.

Such a scheme has been proposed in a patent "Multi-chip OPS laser" filed by Shu at Coherent Inc. in 2014 [46]. The patent described theoretical design for a multi-chip OP VECSEL. The design is very similar to the interferometric setup presented by DiDomenico, with the exception that the gas laser gain medium has been changed to VECSEL. Patent includes theoretical descriptions and discussions of the problematics of such interferometric system, summarizing the experience of previous researches done in this field. For instance, fringe forming, arising from interference between incident and reflected mode, cause spatial hole burning and reduces available power. The benefits of the

approach are single-frequency operation: scaled-up output characteristics that corresponds to the combined power of the two VECSEL chips. Furthermore, with minor modifications and insertion of a non-linear crystal the setup allows second-harmonic generation to visible wavelength.

This section is devoted to the description and discussion of practical implementation of the multi-chip interferometric VECSEL. Information provided here concerns preparation and designing of the experiment, as well as carrying out the experiment.

The Master's thesis experiment has been conducted in Optoelectronic Research Center's optics laboratory at Tampere University of Technology. All safety measures concerning working with lasers and electrical equipment have been followed. The measures include means of personal protection, such as wearing protective glasses, which cover the wavelength range from shorter pump wavelengths up to laser emission wavelengths. Screening of scattered pump light have been done when carrying out the experiment.

4.2 Design of the cavity

Design of the interferometric VECSEL concerns the distances of the optical paths and transverse mode sizes at gain chips. As it was mentioned in Chapter 1, the external cavity should define a cavity mode size on the gain chip that roughly matches with pump beam spot, in order to achieve maximum efficiency and maintaining fundamental transverse mode. Therefore, during simulation of the cavity three main parameters have been taken as constant ones: the pump beam spot on the gain mirror and the distances L_1 and L_2 between gains and output coupler. In such a way all other parameters of the cavity, such as the distance from beam splitter to the output coupler (common arm) and output coupler's radius of curvature have to be received by means of cavity simulation software. As it has been mentioned in Chapter 2, ΔL is the difference between L_1 and L_2 and plays a seminal role in achieving single-frequency operation. Using Eq. 3.8 and assuming that the optical spectrum linewidth is equal to ~10 nm, the upper limit for ΔL is approximately equal to 80 μm. Such small length difference can be neglected in the preliminary cavity design. Thus, for the simplicity it has been taken that $L_1 = L_2 = L$=110 mm. This length is considered to be reasonable taking into account physical dimensions of the setup components.

Figuring out the dimension of the focused beam spot starts from the characteristics of the laser diode pump. Pump's optical system consists of an optical fiber, a collimation lens and a focusing lens. For this experiment a focusing pump lens with a focal length of 16 mm has been chosen. The minimum beam size which can be achieved is defined by M^2 parameter of the laser diode. In the case of pump diodes that have been used in this experiment, the minimum pump beam radius is equal to 150 µm.

Knowing the minimum beam size of the pump beam and distance L, it becomes possible to execute a simulation in order to define other cavity parameters. By means of WinLase computer software, based on ABCD matrix formalism, it was possible to make a simulation of the optical cavity.

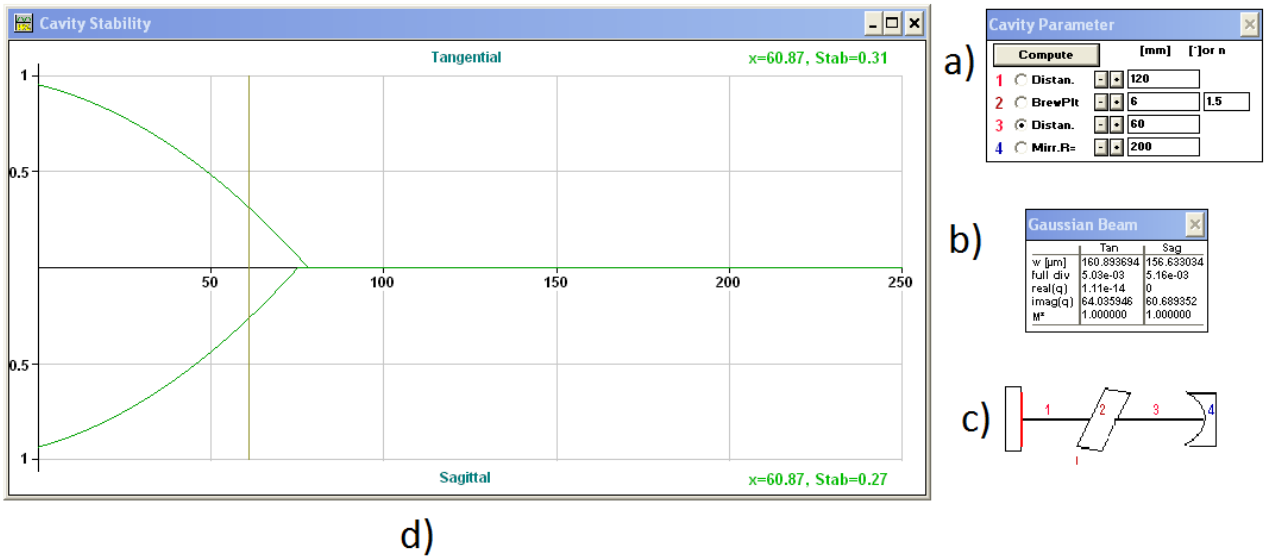

Figure 4.2: Simulation of the laser cavity with WinLase software. a) Cavity parameters, one parameter can be variable; b) Gaussian beam characteristics; c) – scheme of one arm of the interferometric setup. 4 – cavity stability the chosen variable parameter.

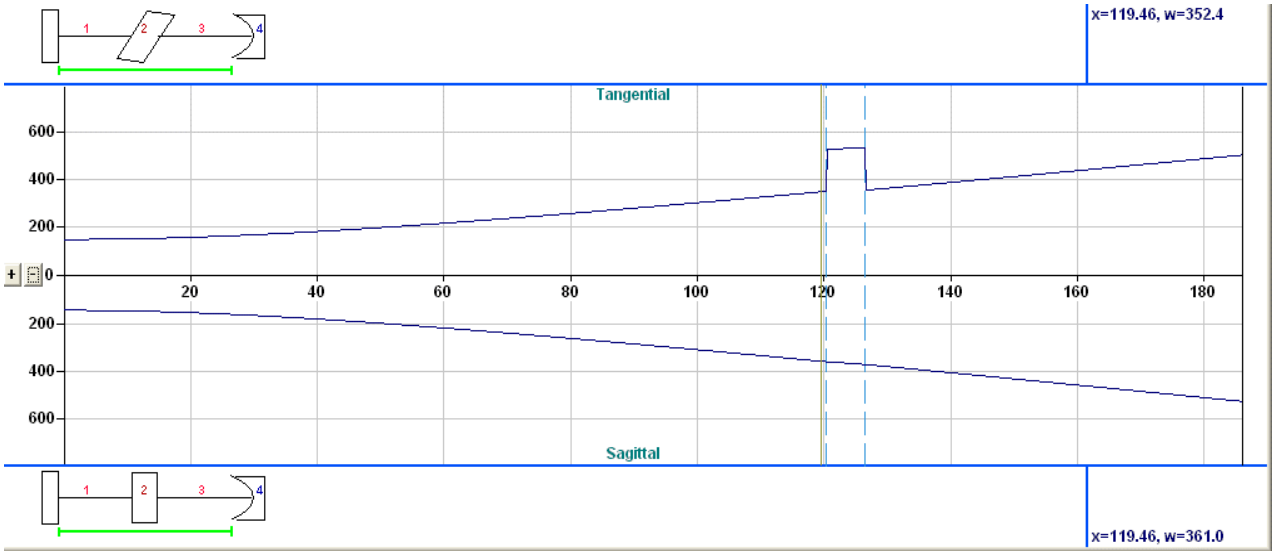

Figure 4.3: Simulation software screenshot, which shows laser beam profile inside the resonator along the entire cavity length; both tangential and sagittal dimensions are shown. Because of BS slight beam ellipticity is introduced.

Taking into account the simulated cavity, the real scheme of the experimental setup was designed and built as shown in Fig. 4.4. Pump tubes hold the optical fiber and direct the incoming 980 nm pump light onto the VECSEL chips at some angle with the respect chips' surface plane. The angle is determined by the focal length of the pump focusing lens and the fact that laser beam must not be blocked by the pump tube. Physical dimensions of the pump tubes are ~100 mm. Taking into account cavity arm's length, focal length of the pump focusing lens and given angles of the pump tubes, one can make a conclusion that it is physically impossible to place pump tubes at the same angles, without their touching. Therefore one of the pump tubes was placed at an angle of approximately 35 degrees, when another pump tube had 30 degrees angle. The tubes had been designed for spherical focusing lenses instead of cylindrical lenses. With spherical lenses the angle of the pump tubes creates an elliptical shape of the pump beam spot on the VESCEL ship, which can lead to additional losses of the pump power even under the condition of a perfect mode matching.

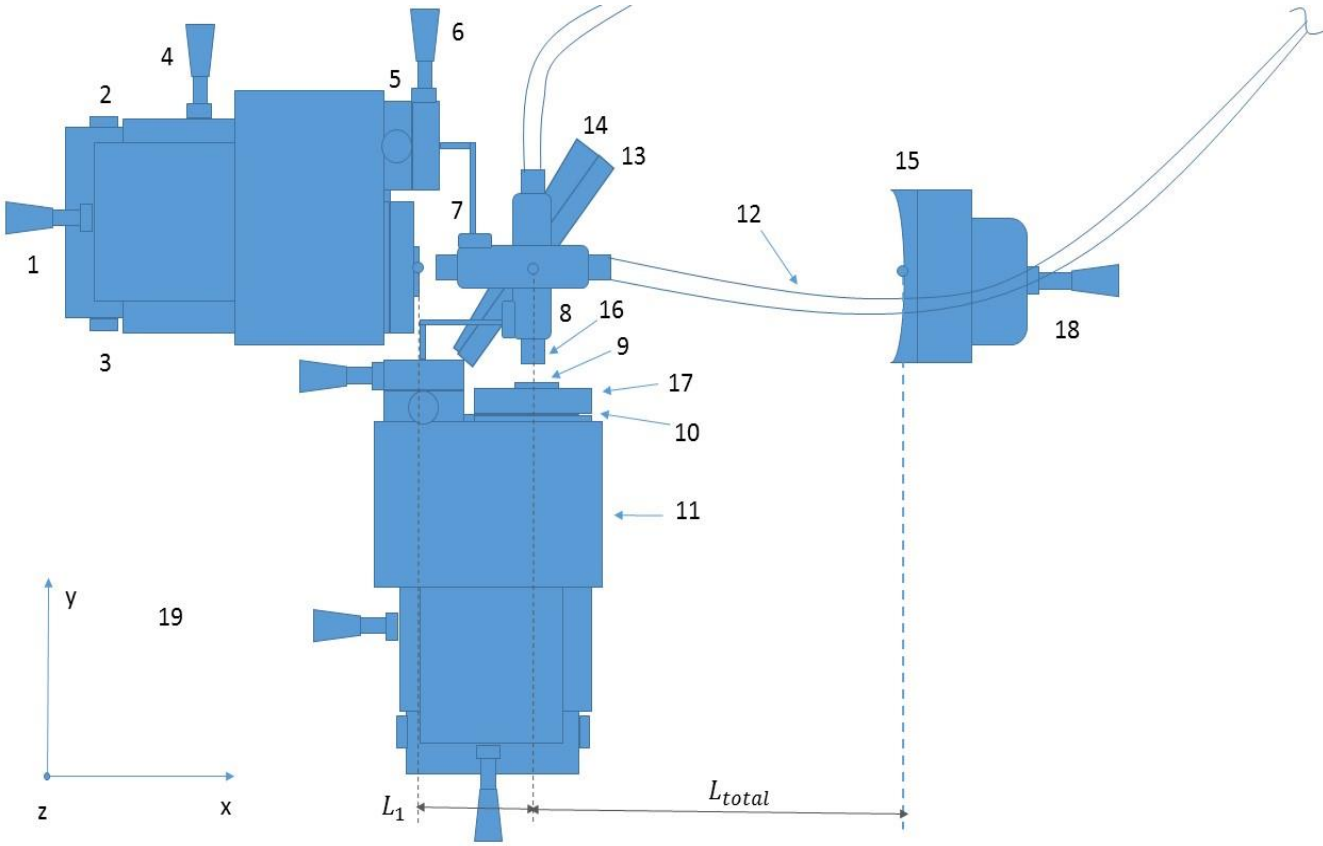

Figure 4.4: The main components of the two-chip laser setup: 1-linear stage for displacement in x-direction; 2-knob for tilting in x-y direction; 3 knob for tilting in x-z plane; 4- linear stage for displacement in y-direction; 5-knob is for displacement of pump tube along z-axis; 6- knob for a displacement of pump tube along y-axis; 7-linear stage for focusing pump light; 8-pump tube; 9-VECSEL chip; 10- thermoelectric cooler; 11- heatsink; 12-pump's optical fiber; 13- beam splitter coating; 14- AR coating; 15- output coupler; 16-pump focusing lens; 17- copper sub-mount; 18- linear stage for displacement of output coupler along x-direction; 19- optical table;

4.3 Components of the setup.

Experimental setup's components can be categorized as follows: mechanical components, optical components, optoelectronic components and electrical components. The mechanical components of the laser setup include mechanical stages and mounts provide linear and angular displacement and maintain fixed position of objects. The translation stages provide displacement with a precision of hundreds and even tens of μm.

The mirror mounts guarantee an angular displacement along two axes with the precision of arcminutes.

The optical components comprise the following items: beam splitter, DBR mirror, output couplers, collimating and focusing. The beam splitter plate had a dielectric coating dielectric coating with 50/50% transmittance-reflectance ratio when being placed at an angle of 45 degrees with the respect to the incident beam. The backside of the splitter plate was AR coated. The coatings were designed specifically for IR light in the wavelength range from 0.9 to 2.6 μm. The AR surface has a 30 arcminutes wedge relatively BS surface [46]. Output couplers with coupling ratios of 0.7% and 2.5% have been used. Both of these couplers have 200 mm radius of curvature according to the cavity design parameters and working wavelength range of ~ 300 nm.

The optoelectronical components of the setups are the two VECSEL chips and two pump diodes with operational wavelength of 1.27 μm [48].

Diode pumps work as optical power sources for the both of the chips. There are not strict limitations for choosing the pump, except that it should generate shorter wavelength than operational laser wavelength than the absorption edge of the AlGaInAs barrier and spacer layers of the VECSEL gain structure. The structure described in section 2.4. absorb wavelengths below ~1μm. Taking this into account two commercial laser diodes with operational wavelength of 980 nm and maximum optical power of 70 W have been choosen. These pumps are electrically driven by a voltage-current source. Pump lasers are cooled by a water-cooling system.

Electrical components laser diodes drivers, thermoelectric cooling elements, laser pointers, powermeters, photodetectors. Electrical drivers are convenient tools for adjusting and regulating the device outputs. For instance, light-current characteristic (L-I curve) of the laser diode pump has next form:

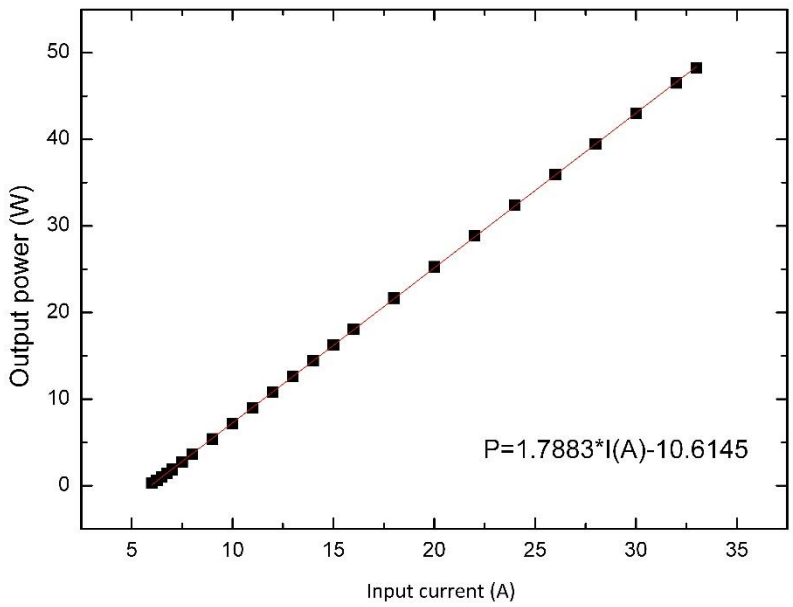

Figure 4.6: Current versus output light power dependence of the pump laser diode. Formula for transferring ampere values into optical watts is given (formula is fair for the medium operational powers).

For the efficient cooling of VECSEL chips during laser operation, two thermoelectric coolers (TEC). TEC exploits Peltier effect. Peltier effect occurs when DC voltage is applied to n-type and p-type semiconductors. Array of semiconductors are placed thermally in parallel and electrically in series, so that applied DC voltage cause a DC current. Current flowing through the semiconductors leads to temperature difference. Thus, TEC has two sides: hot and cold. VECSEL chips are attached to the cold sides, when hot sides of the TECs are attached to the heatsinks. Extracting the heat from the hot side leads to a bigger efficiency of TEC. TEC is driven by means of electrical driver, which regulate the current, and maintains the set temperature.

Besides the above-defined components building and aligning the setup requires many accessory devices. Such as a beam profiler camera, IR sensitive digital microscope and detector, optical intensity measuring thermal heads, an optical spectrum analyzer, and an electrical spectrum analyzer.

4.4 Operational, alignment and measurement techniques

In order to have a working laser system a precisely aligned optical cavity is required. In other words, the spontaneous emission light emitted from the VECSEL chip should be guided through the cavity so that it will replicate its path during round trips, which number tends to infinity, causing stimulated emission. The adjustable mounts of the optical components provide precise alignment capabilities. Mounts that hold the VECSELs, provide six degrees of freedom and additional three degrees are available for the pump beam light.

Alignment of the setup should be started from the alignment of the pump beam on the surface of the gain chip. Due to imperfections from processing of the chip, which cause the chip surface to be uneven and which lead to differences in laser performance when moving pump spot across the chip's area, appropriate pumping region has to be found. Therefore, for the simplicity of the alignment, the appropriate spots on the chip surfaces should be scrutinized in the simplest linear cavities. Thus, two linear cavities with VECSEL mirror and a curved output coupler have been built (Fig. 4.1 (a). In each cavity, moving the position of the pump tube across VECSEL chip and matching the cavity mode for this spot by means of output coupler adjusting, the best regions for lasing have been chosen. Example of such region can be seen in the photo shown in Fig. 4.7.

After the alignment of the pump beam on the VECSEL gain element surface, position of the pump tubes remain constant relatively gain surface, because of their rigid connections to the heat sink. The assembly, which has been particularly designed and implemented in this setup in order to simplify following the alignment process, allows to move the whole mount chip and heatsink in all possible degrees of freedom without losing the appropriate lasing region.

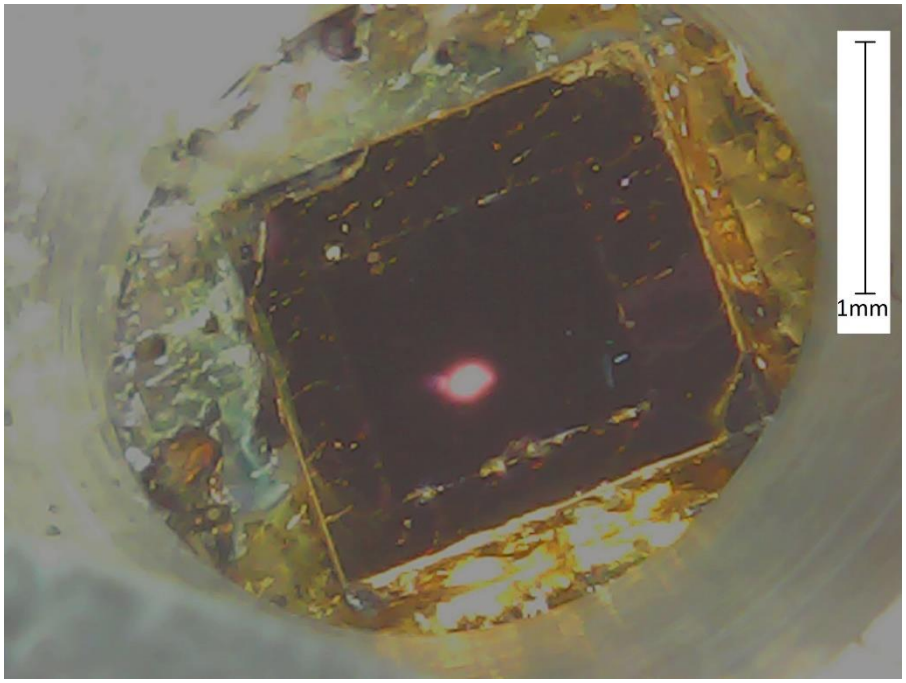

Figure 4.7: Photo of the VECSEL chip and pump beam spot incident onto the region giving the best performance. The 980 nm pump light can be seen with a digital microscope sensitive in the IR spectrum. The focused pump beam has a radius of 150 μm.

Alignment process can be considerably simplified by using a laser pointer of visible wavelength in the prealignment stage. The pointer simulates the laser beam path in order to make a rough alignment of the optical components in the setup. The differences in refraction between pointer light and laser light can be neglected or compensated by further fine alignment. However, it can be more reasonable to use a pointer with a wavelength which will not be efficiently absorbed by the laser gain material and which can be reflected by the VECSEL's DBR.

Simple illustration of linear cavity alignment by a laser pointer can be seen in Fig. 4.8.

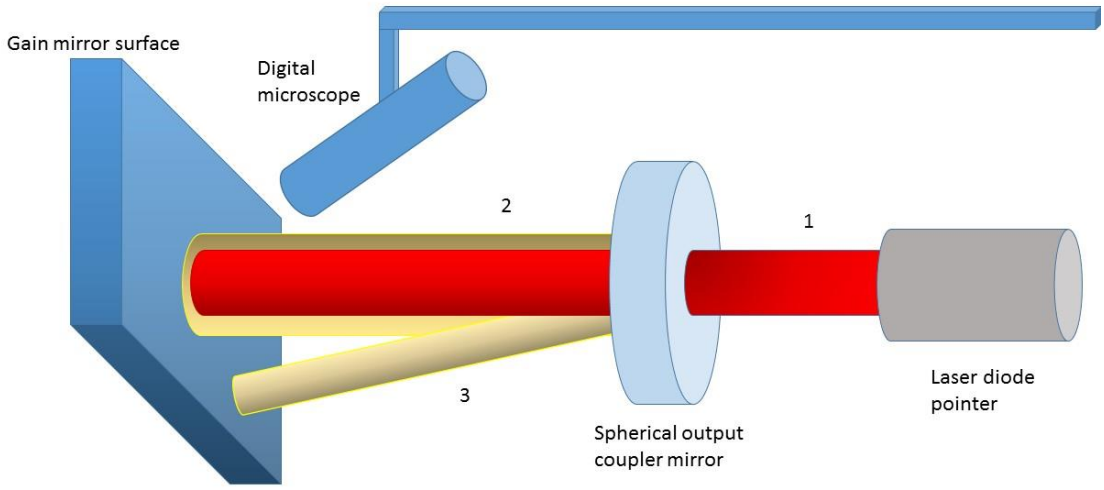

Figure 4.8: Technique for cavity alignment. Firstly, the VECSEL gain mirror surface is adjusted exactly perpendicular to the incident pointer beam. The surface reflects the beam exactly back to the pointer (1). Then the coupler is placed at the proper distance, so that the pointer beam will hit the center of the mirror. The coupler must be placed so that the pointer light refracted by the coupler will hit the same spot on the gain mirror as it hits without coupler. Light passes through the coupler then becomes reflected from the gain surface, and returns to the coupler (2). Part of the light returns back to the pointer and part of it returns to the gain (3). When the beam #3 reach the surface it is relatively dim, but a digital microscope can be used to spot it. After adjustment of the output coupler mirror, when beam #3 coincides with the beam #1 on the gain surface, the alignment can be considered as achieved. After that, only small changes need to be done to make the system lase.

When the pump tubes have been aligned aligned towards proper gain area, it is possible to proceed further building the interferometric multi-chip setup. Gain chip's mounts are placed at the proper distances between each other and BS. By default it is taken that gain mirror surfaces are perpendicular to the optical plane. Beam splitter is placed so that it reflects the incoming pointer beam towards the gain element in the perpendicular arm of the multi-chip cavity at an angle of 45 degrees. Dielectric coatings of the beam splitter have not been designed for pointer wavelength. Due to this fact, multiple reflections from

beam splitter become produced. In order to choose the right beams, the following scheme for the setup alignment has been made and followed:

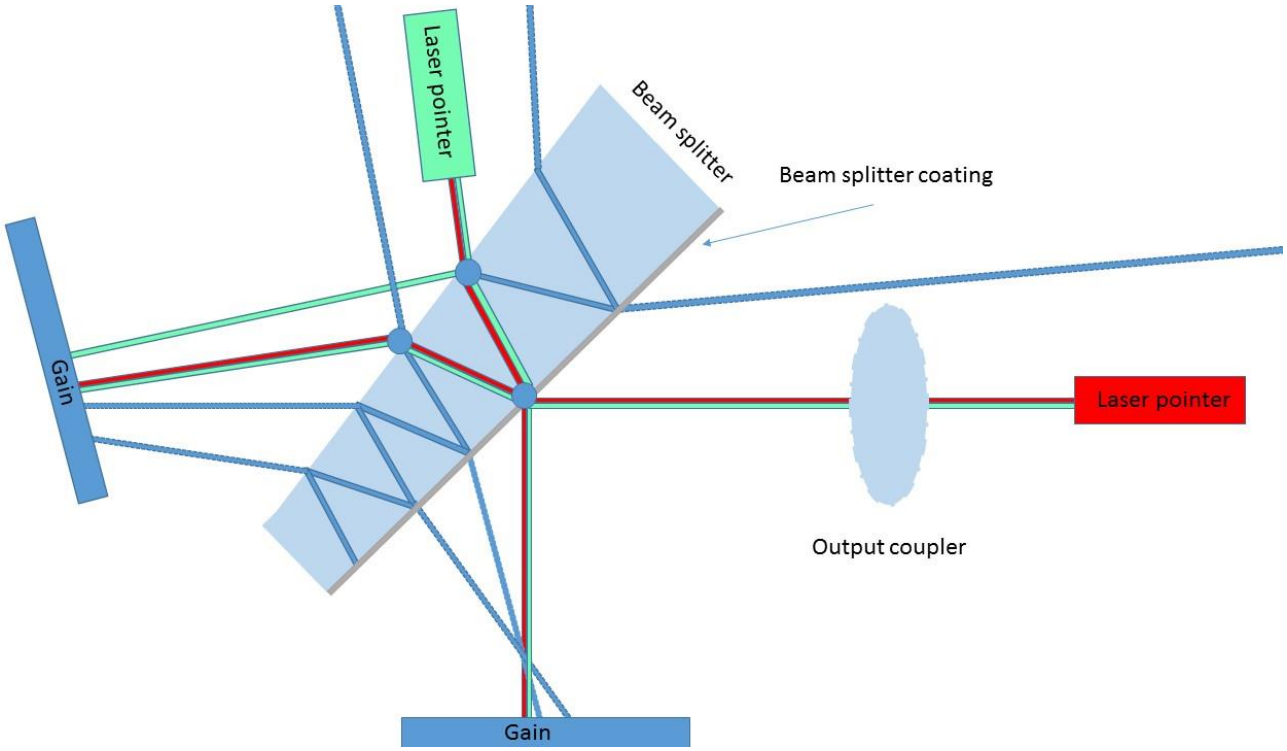

Figure 4.9: Scheme of light beams produced by beam splitter because of internal reflection. Blue lines represent parasitic reflections that should not be followed.

Fig. 4.9 must be followed in order to make the aligning possible . Otherwise, multiple beams from the beam splitter can be confusing and lead to wrong adjustment of the cavity. The alignment process of the interferometric cavity can be done using two pointers with different wavelengths. At the first stage after placing the gain mounts at the proper distances, a green pointer should be placed so that its light will hit the beam splitter coating, as shown at the picture. After properly orienting the gain mirrors, green light will duplicate its path and return to the pointer. After that red laser pointer has to be placed at the position of incoming green light from the side of the AR coating of the beam splitter. The red laser pointer should be thoroughly aimed so that its light will replicate the light path of the green pointer. The main idea of implementation of the green pointer is that it makes it possible to insert the output coupler inside the cavity and detect the light reflected from it. This light will be used to align the output coupler, and finally complete the rough

alignment process. Otherwise, if the coupler will be put inside the cavity when only one green pointer is used, it will be impossible to track the reflection from the coupler, because of the much longer optical path and the consequent losses the light will experience.

After laser pointer alignment, fine alignment technique should be carried out using photodectors to track the spontaneous emission level during aligning. Filters are used to screen the detector from scattered pump light. The stability of the interferometric laser was found to be very low, i.e. even little deviation of light from its ideal path in the cavity will immediately lead to losses overcoming the gain.

After lasing has been achieved and the laser performance has been optimized, several issues come up regarding the laser operation. First of all, as it has been mentioned before, optical pumping causes a raise of chips temperature, and therefore, the gain chip has to be efficiently cooled down. Usually, water-cooling is applied. Disadvantage of the water-cooling is acoustical vibrations caused by the water pump, which can have an impact to the laser operation regime. Since the interferometers are extremely sensitive devices to any kind of vibrations, all possible sources of mechanical vibrations should be avoided. A thermoelectric cooler has been applied as a cooling device in this setup. Even though, TEC provides no mechanical vibrations, but the cooling capability can be quite limited. TEC's basic principles of operation assume cooling down one side, to which VECEL's substrate is attached, and heating up the opposite side. The temperature difference between the cold and hot side has to be maintained as small possible for better efficiency. Therefore, hot side should be connected to a heat sink, which has a relatively big thermal. However, the heat sink thermal capacity is limited by its size and weight. Weight is a crucial parameter for the all translational and rotational mounts which hold the heat sink and the VECSEL chip mounted on it. Too much weight can cause jamming and instability of the assembly. The heatsink chosen for the experiments can maintain a sufficient temperature difference for approximately 15 minutes at medium pumping power before overloading of the device.

Measurements of the laser setup include the defining the M^2 factor of the laser. M^2 factor is the beam quality factor of a laser beam. Beam quality factor shows by how many times laser beam is bigger than a diffraction limit for a particular wavelength. The smaller M^2 factor, the tighter beam can be focused. For the fundamental Gaussian beam with transverse intensity profile, M^2 defines as follows

$$I(x,z) \sim \exp\left[\frac{-2x^2}{w^2(z)}\right]. \quad (4.1)$$

The transverse beam size parameter w=w (z) varies in z-direction as [49]

$$w^2(z) = w_0^2 + \frac{\lambda^2}{\pi^2 w_0^2}(z - z_0)^2, \quad (4.2)$$

where w_0 is the minimum beam size which corresponds to z=z_0, λ corresponds to the operational wavelength.

The real-beam transverse size for the taken laser beam can be described as follows [50]

$$W_x^2(x) = W_{x0}^2 + M_x^4 \frac{\lambda^2}{\pi^2 W_{x0}^2}(z - z_{0x})^2 \quad (4.3)$$

where W_{x0} is the minimum transverse real-beam size under certain z_{0x}. The analogous equation can be obtained for a y-transversal-direction.

For an ideal Gaussian beam M^2 factor is equal to one.

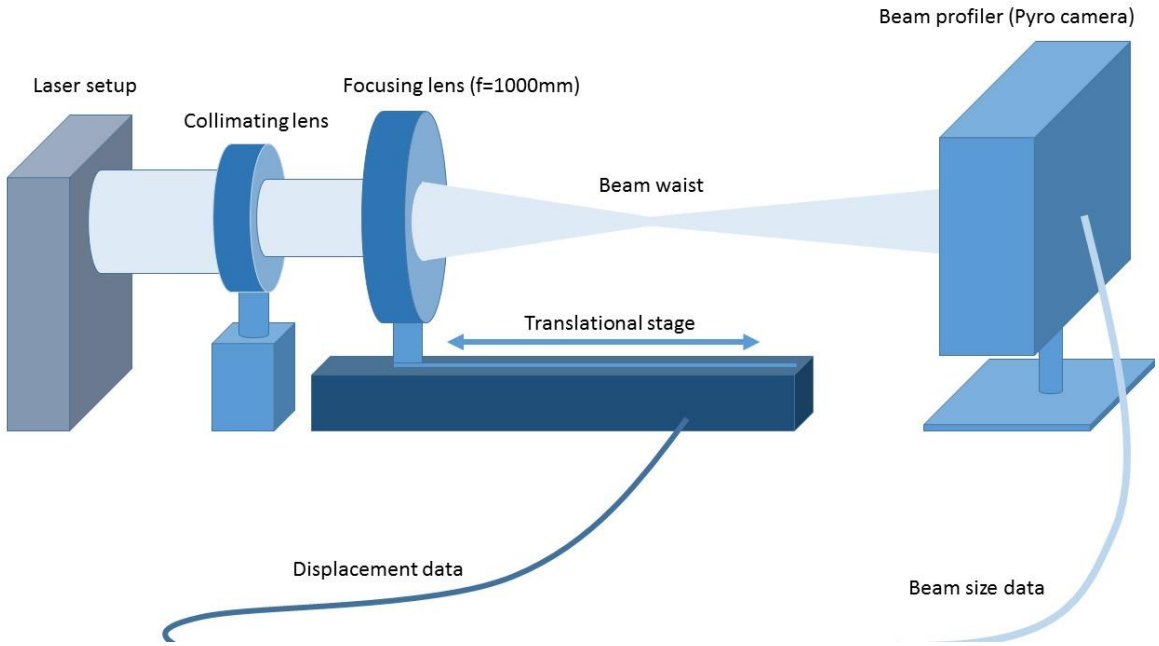

Figure 4.10: Setup used for the M^2 measurements.

By means of Eq. (4.3) M^2 factor of a particular laser can be experimentally determined. The M^2 measurements can be implemented by means of the setup showed in Fig. 4.10. A beam profiler measures the transverse beam size at different positions along the beam waist. It is implemented by means of translational stage on which the focusing lens is placed. The displacement and beam sizes are recorder. By means of fitting the experimental data with Eq. 4.3, M_x^2 factor, minimum waist size W_{x0} and its location z_{0x} can be derived.

4.5 Problematics

One of the main challenges of the two-chip interferometric VECSEL setup is acoustical vibrations. Taking into account the considerable level of sensitivity, which is a feature of almost all interferometers, the presence of mechanical vibrations can have a significant impact on the laser operation. Noise vibrations can result in pulsations of the output power, initiation of parasitic laser modes, and changes in the optical path. The laser setups was built on optical table, which is supposed to dump any external impacts and vibrations. Nonetheless, such and air-cushioned table did not prove itself as a satisfying enough measure for preventing the above-mentioned negative consequences of vibrations. Moreover, not only acoustic vibrations have negative influence on the laser operation, but any disturbances of the air medium inside the cavity, lead to changes in the optical path inside the cavity and provoke instabilities similar to those caused by mechanical vibrations. In order to get rid of these negatives effects the decision to isolate the setup by placing it into a sealed box was made. The results are available in the Chapter 5.

Moreover almost all mechanical mounts which hold the chips and pump tubes in place have limited durability. Big weight of the components, such as heat sink and other components, decreases stability of the translational and rotational mounts on which this weight has been placed. The mounts under such conditions are unable to provide smooth and continuous displacement. This makes it very hard to achieve enough precision for the alignment. In addition, mounts holding big weight cannot provide enough long-term stability, which means slow degradation of the initial mount position with a time. Therefore, the laser setup demands additional realignment after some period.

Taking into account above-discussed imperfections of VECSEL chips and low stability of the optical system, the alignment process becomes a hard task. The setup has a poor gain, which means that the laser cannot withstand additional losses.

Initial broad spectrum linewidth of the multi-chip setup puts stricter condition for the achieving the single-frequency operation.

All these above-mentioned issues make it hard to achieve a stable operational regime, and affect many laser parameters such as beam quality and optical spectrum linewidth.

Chapter 5

Experimental results

5.1 Single chip experiments

This Master's thesis work aimed at achieving single-frequency operational regime by means of intracavity interferometric frequency filtering. Furthermore, the experiments investigated power scaling by means of coherent combining of the multiple VECSEL chips.

As it has been mentioned earlier, the presented laser setup consisted of two different VECSEL flip-chips operating at the wavelength 1270 nm. The one can consider it consistent to start from the descriptions of these chip's characteristics.

Figures show power characteristics of both chips. Input power is the incident pump power.

Both chips were investigated under the same conditions and in the same cavity designs (Fig.4.1(a)). Chip's temperature was maintained to 15 degrees. Pump beam was focused to the 150 μm. Output coupler has radius of curvature equals to 200 mm and the reflectivity of 97.5%. Pump angles are 35 degrees and 40 degrees correspondently.

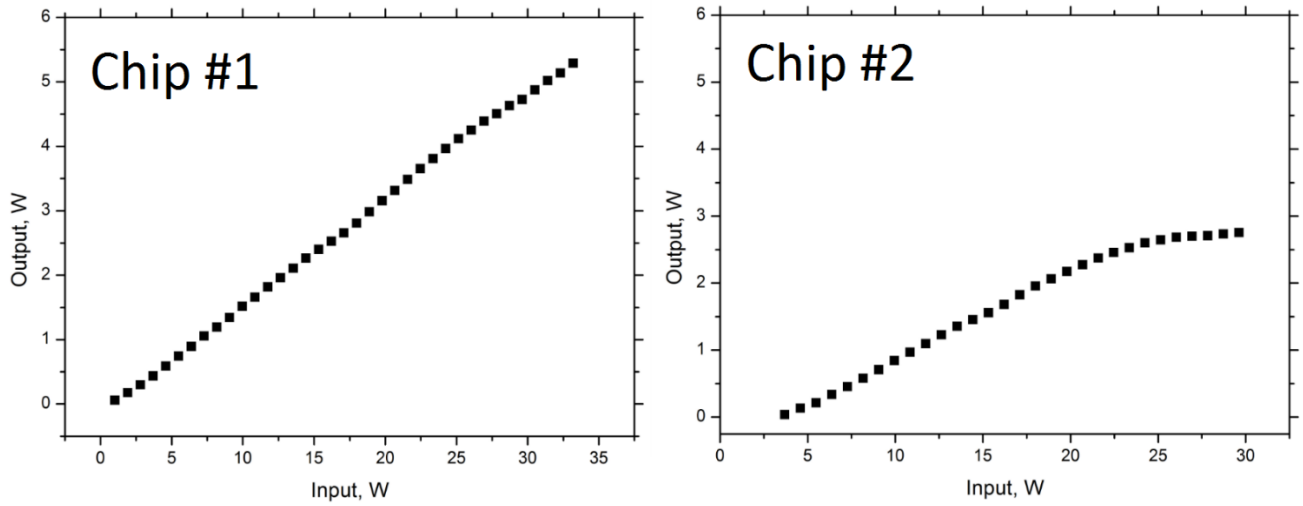

Figure 5.1: Light-light dependence (L-L curve) of the VECSEL chip #1 and #2.

Output optical spectrum of chip #1 and #2 measured with an optical spectrum analyzer can be seen in Fig. 5.2:

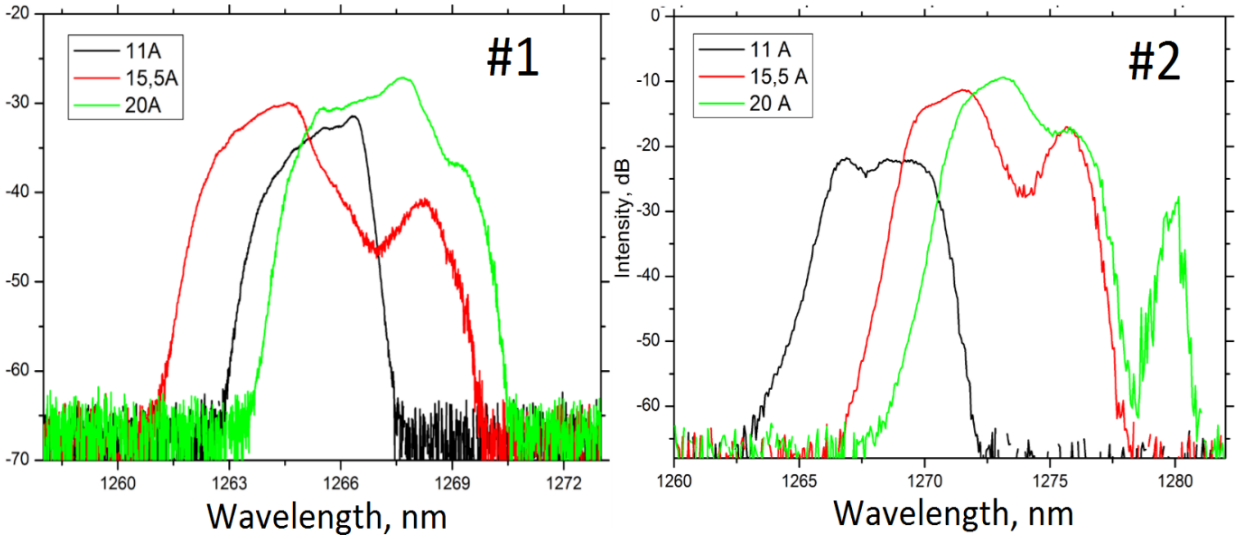

Figure 5.2: Optical spectrum of the chip #1 and #2 at the different levels of pump powers. Chip's temperature has been maintained at 15 degrees by TEC current controller.

As it has been mentioned in Chapter 2, increasing of the incident pump power leads to changes in output spectrum due to thermal and quantum effects. Following output spectrum characteristic in Fig. 5.3 shows spectrum dependence on the different temperature values, when the incident optical power was constant and equaled

approximately 16.21 W. Technique of slight spectrum shifting by means of temperature changing can be useful for matching the output wavelengths of the two VECSEL chips.

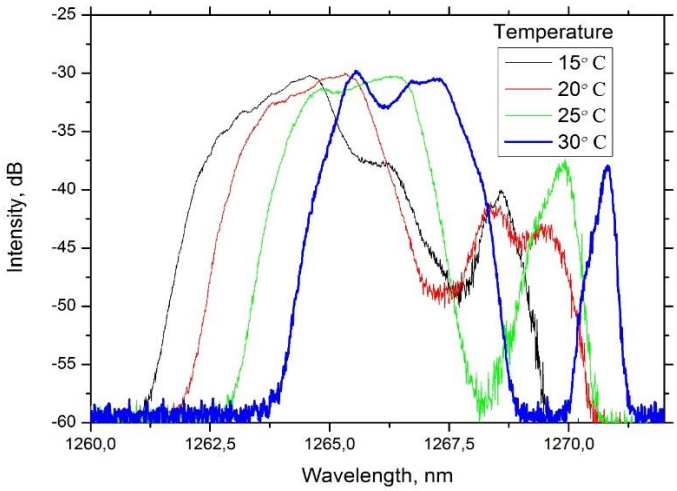

Figure 5.3: Optical spectra of the chip #2 taken with constant pump power at different chip's temperatures. Pump current equal to 15 A.

5.2 Interferometric setup

After the laser setup has been properly aligned and optimized, multiple output beams are generated. They are marked as follows:

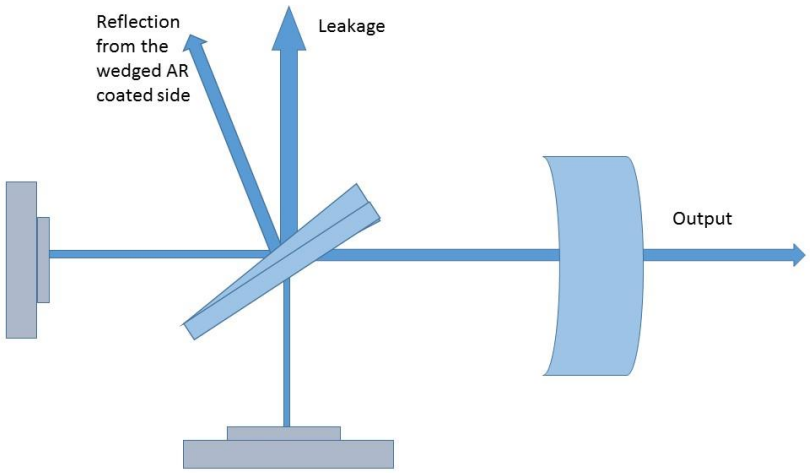

Figure 5.4: Laser output beams. The output beam emitted through the output coupler is considered to be the main one. The leakage of the setup depends on the interference rate and frequency matching. Reflection from the AR coated wedged side of the beam splitter

can be observed, even though power values of this reflection does not exceed 5% of the total sum of leakage and main output, and therefore can be neglected.

The power characteristics of the laser were measured with a thermal powermeter. The light-light curve of both the outputs the main one and the leakage (Fig. 5.7, Fig 5.8). The maximum output power before thermal roll-over is 3.7 W, leakage is 1.27 W. For the setup with output coupler with 0.7% coupling ratio maximum output is 2.6W , leakage is 1.3W. As it can be seen, maximum output of the multichip setup does not exceed the output of single-chip setup.

The beam profile of the output laser beam was investigated by means of a pyrocamera, which allows displaying the beam intensity distribution together with the beam size parameters. The same camera also has been used in M^2measurements. Figure 5.5 shows the beam profile picture received from the camera. Changing the coupling ratio of the output coupler from 2.5% to 0.7% coupling ratio brought the significant differences in the beam profile picture (Fig. 5.6).

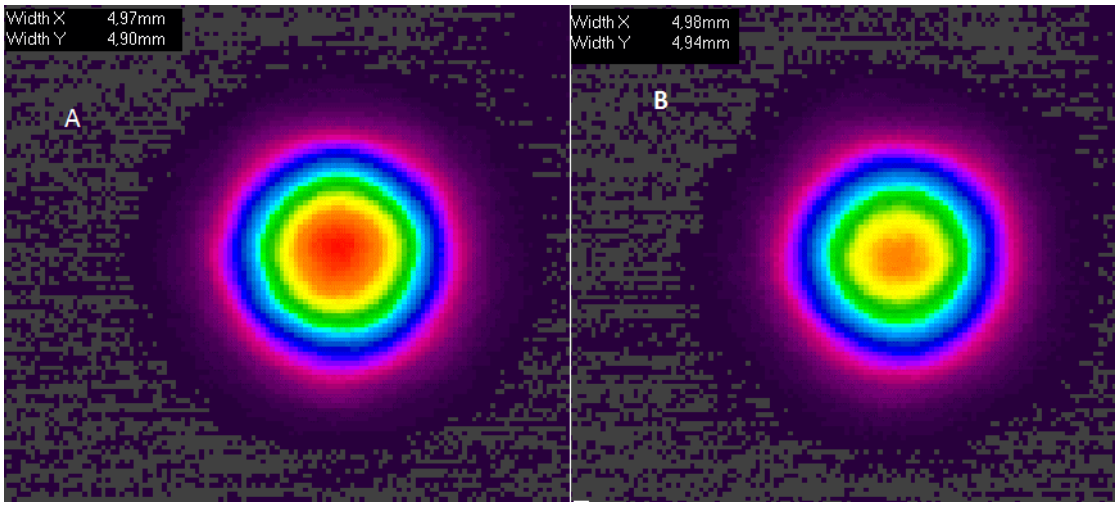

Figure 5.5: Laser beam profile images for various pump powers: a) corresponds to 23 W; b) corresponds to 11 W. The beam profile is very close to fundamental Gaussian intensity distribution. The laser cavity has been equipped with 2.5% output coupler.

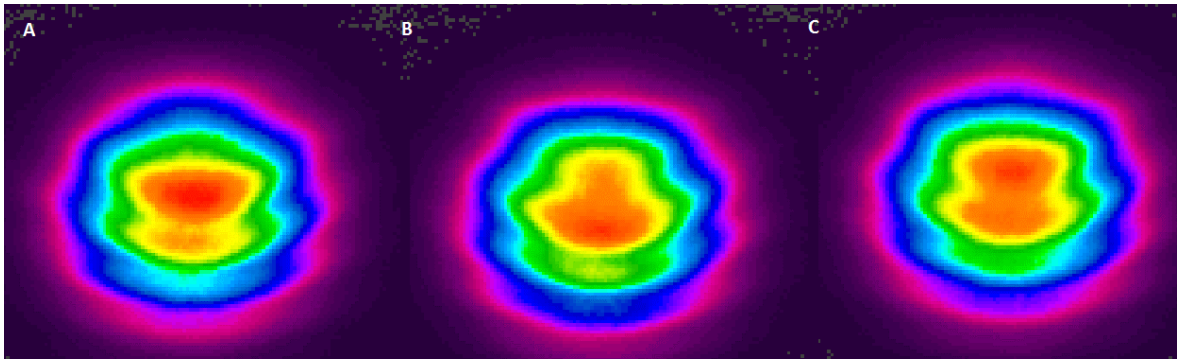

Figure 5.6: Laser beam profile pictures taken at the pump power of 17 W. Optical cavity was equipped with 0.7% output coupler. Three pictures have been taken under the same conditions but at the different time moments. These pictures give evidence of the generation of high-order transverse modes and the presence of vibrations, which cause it. Varying mode pattern can be seen from these three pictures

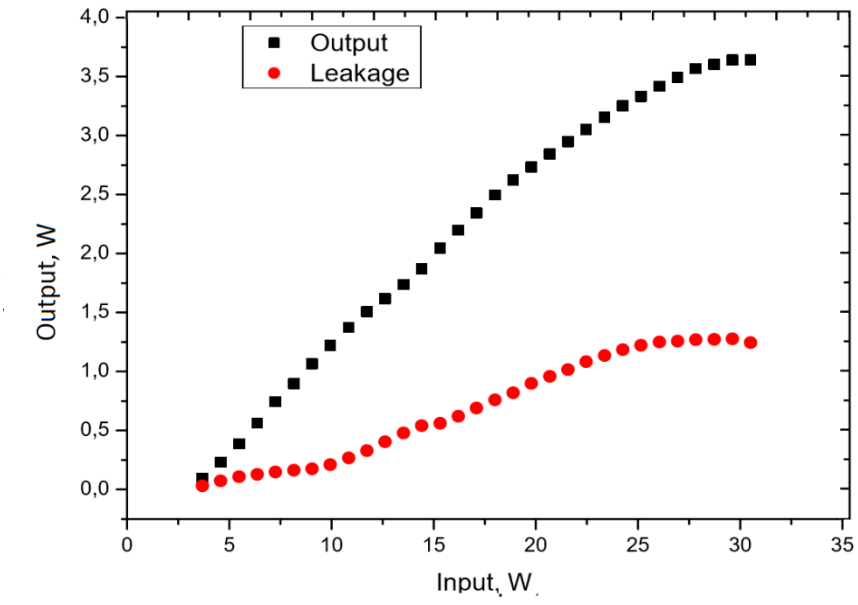

Figure 5.7: Power characteristics of the interferometric setup (L-L curve). The coupling ratio of the output coupler is equal to 2.5%. Two thermal power heads have been used to measure the outputs simultaneously. The chips temperature set to 15 degrees.

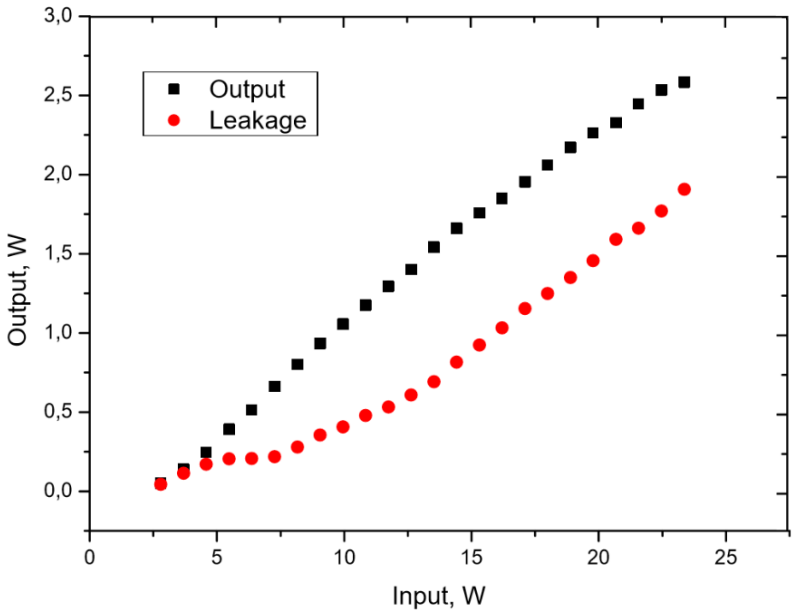

Figure 5.8: Power characteristics similar to the Fig. 5.7 but with the OC mirror with 0.7% coupling ratio.

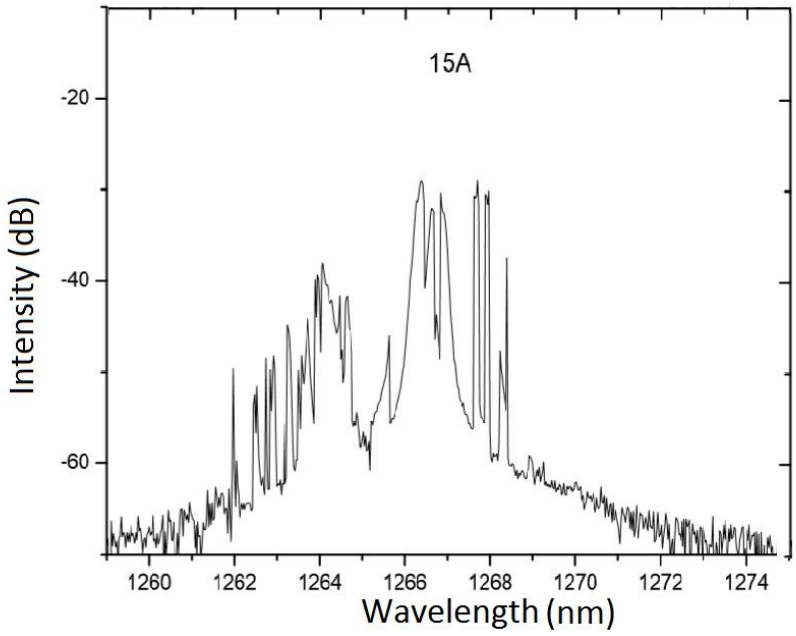

Figure 5.9: Optical spectrum of the setup taken at random value of ΔL. Because of this, many peaks with small separation between each other can be seen. That small separation

distance serves as an evidence that at this stage ΔL was far away from desirable value for single-frequency operation.

In order to achieve single-frequency operational regime, certain ΔL value has to be achieved. It requires fine tuning of the translational stage on which the chip mount has been placed. If the setup is built with the care it is possible to move one mount along the light path without any changes in the beam path. Changing the distance of the perpendicular arm length has been done during the laser operation while simultaneously tracking the output. The output has been investigating by means of an optical spectrum analyzer and radio frequency analyzer (RFA) simultaneously. It became possible by means of a fiber coupler, with approximately equal splitting ratio, dividing signal into two optical fiber outputs. Fig. 5.10 shows optical spectrum near single-frequency operation, FWHM of the optical spectrum is less than 1 nm.

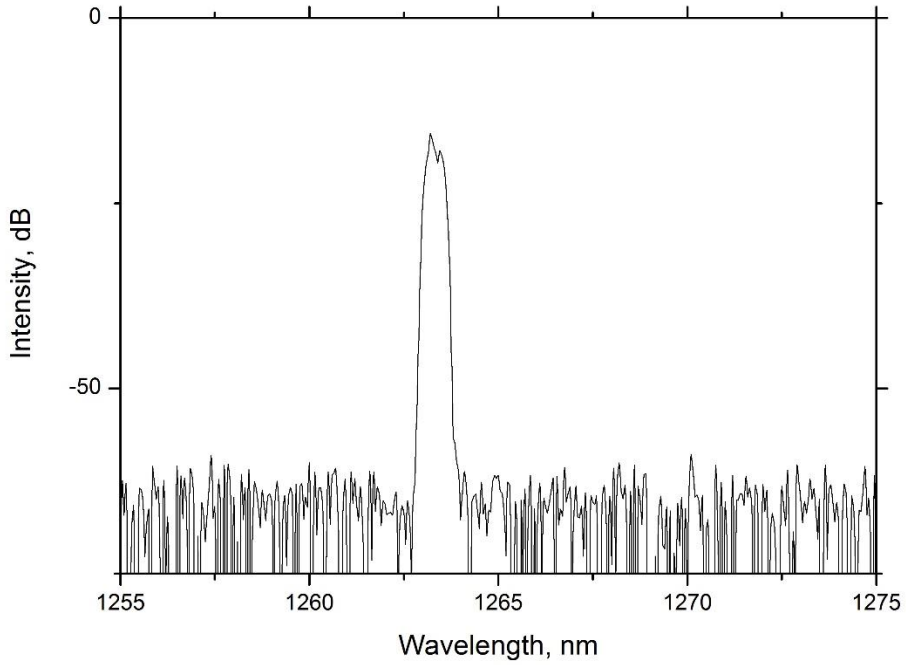

Figure 5.10: Optical spectrum of the two-chip interferometric VECSEL near single-frequency laser operation, when majority of the frequency modes within the gain bandwidth are suppressed.

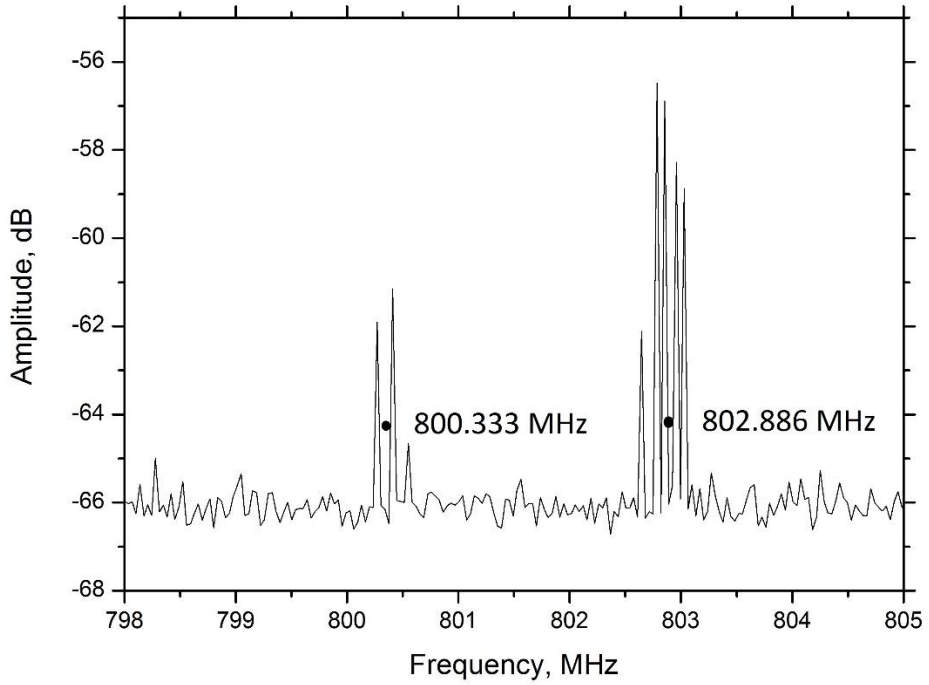

Figure 5.11: Radio frequency spectrum at ΔL near single-frequency operation

By means of RF spectrum it is possible to precisely calculate the real ΔL. RF peaks represent a number of round trips across the cavity that photons do per one second. Therefore, RF spectrum can be transferred into the length of the cavity. The peaks in Fig.5.11 represents signals generated in two cavities: perpendicular arm and common one. The frequency difference corresponds to the length difference in these two cavities. Thus, ΔL difference equal to:

$$\Delta L = \frac{c}{2f_1} - \frac{c}{2f_2} = 110\ \mu m. \qquad (5.1)$$

This value is very close to the previously received theoretical value of ΔL (80 μm).

In order to demonstrate how the length difference ΔL affects the the operation regime of the laser, the output spectrum has been measured for various length differences.

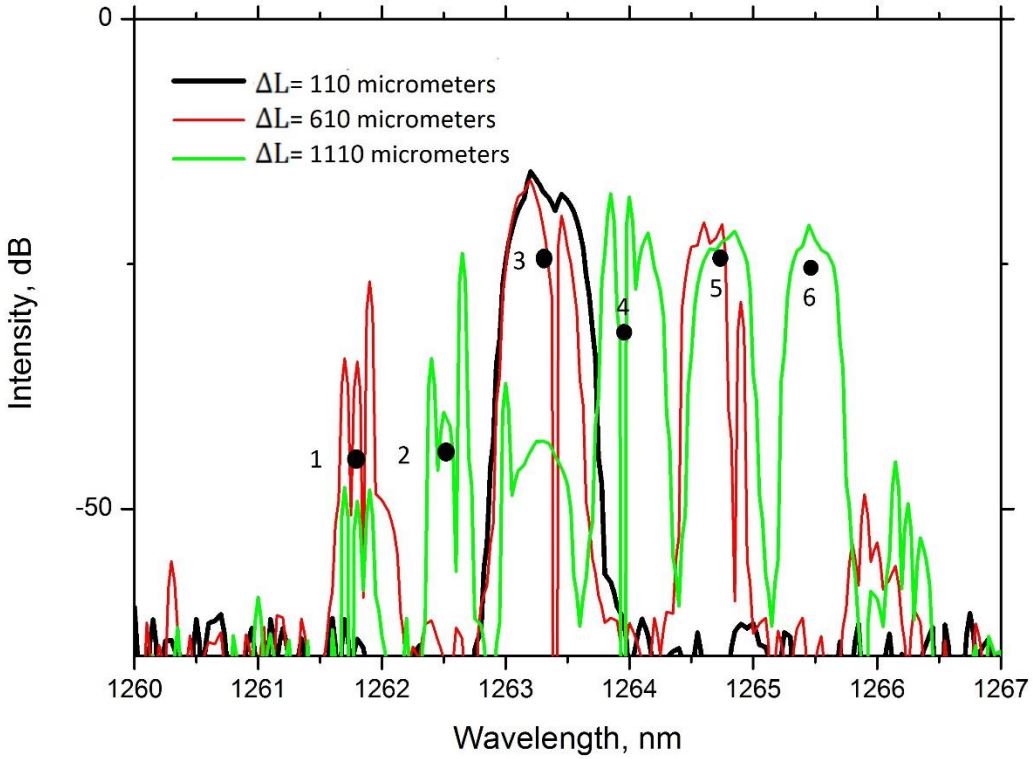

Figure 5.12: Output spectra for different values of ΔL.

Points: 1) 1262.775; 2) 1262.501; 3)1263.375; 4)1264.0389; 5)1264.773; 6)1265.4886 nm.

Thus, increasing the ΔL leads to appearance of unwanted frequency modes, as it was mentioned in the theoretical part.

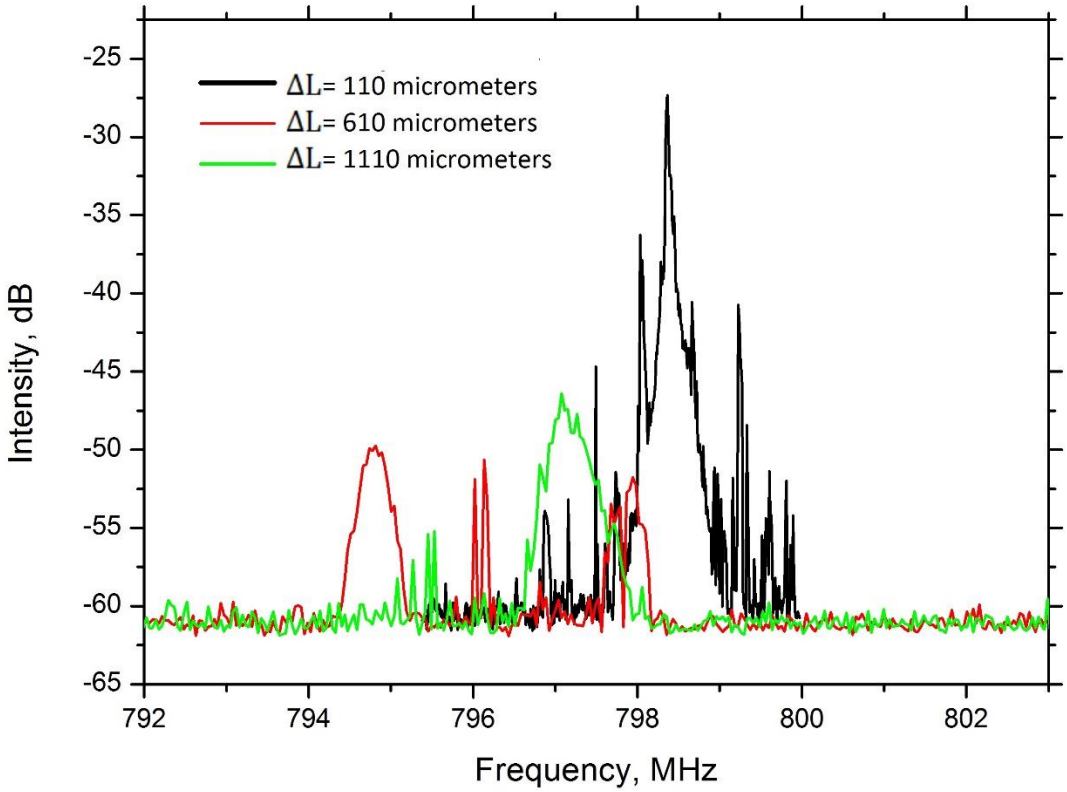

Figure 5.13: Shifting of the radio frequency peaks with a changing of ΔL.

One obvious problem of the laser setup is the presence of acoustic vibrations and airflow inside the cavity. In order to get rid of these negative effects and their consequences the setup has been built from the scratch and placed into special box. A soft cellular body insulating material covers the box from the inside in order to dump the mechanical and acoustic vibrations. In addition, the box was placed onto an same optical table and additionally insulated from it by means of the same cellular body. The laser setup was supposed to work inside the closed box with only one optical fiber coming out from it. Thus, no airflow should be inside the optical cavity and therefore no refractive index alteration. The experimental data in Fig. 5.14, 5.15, 5.16 duplicate the previous measurements with the exception that they were obtained from inbox setup.

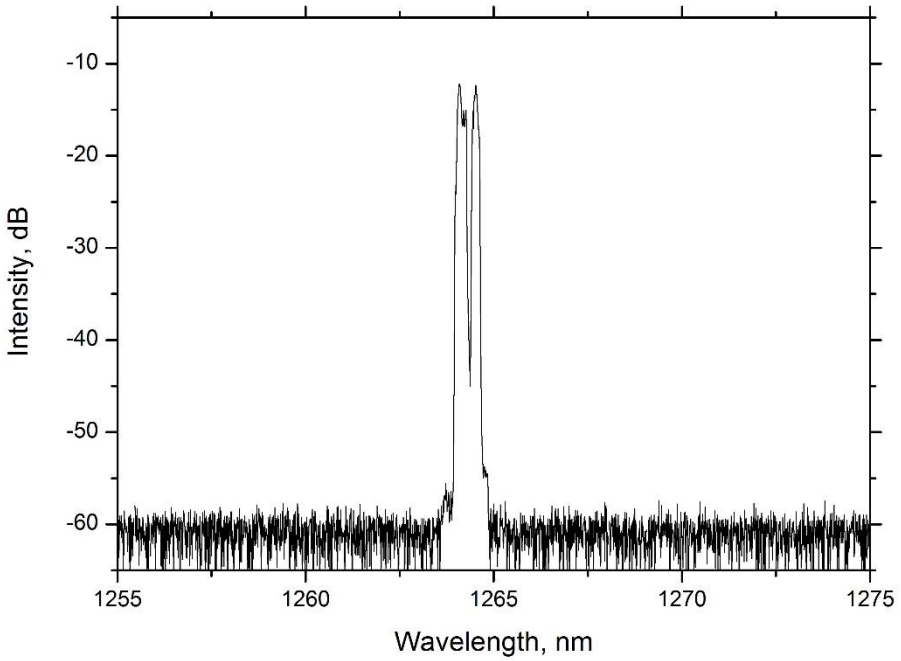

Figure 5.14: Optical spectrum of the inbox setup.

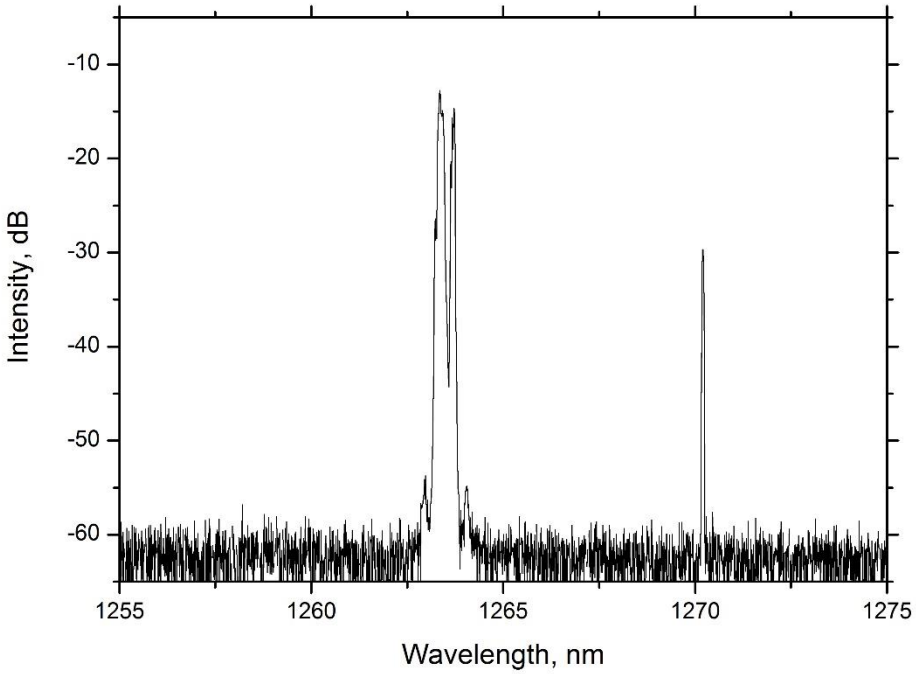

Figure 5.15: Optical spectrum of the inbox setup.

As it can be seen from the Fig. 5.14 and Fig.5.15, the output spectrums remain unstable. Other frequency modes appeared. The mode suppression rate is not strong enough for the big pumping values. The linewidth of the output spectrum has not become any narrower.

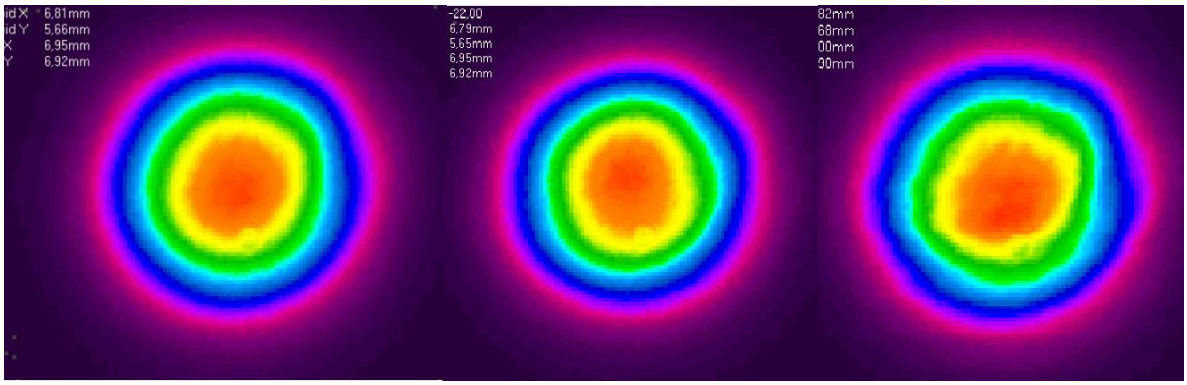

Figure 5.16: Beam profile pictures for the setup built in an acoustically mechanically isolated box, taken at the different time moments. The varying mode patter can still be seen.

Regardless of an attempt to isolate the setup from external vibrations and airflows, the beam profile in Fig. 5.16 gave evidences of vibrations still present. However the magnitude of the vibrations became lower.

In order to demonstrate the two VECSEL chips are participating in the lasing action, a balance test for the chips was done. Power characteristics for the two-chip interferometric VECSEL have been recorder while varying only one pump laser at a time, as shown at Fig 5.17 , 5.18. The other pump was kept at the threshold power of the VECSEL.

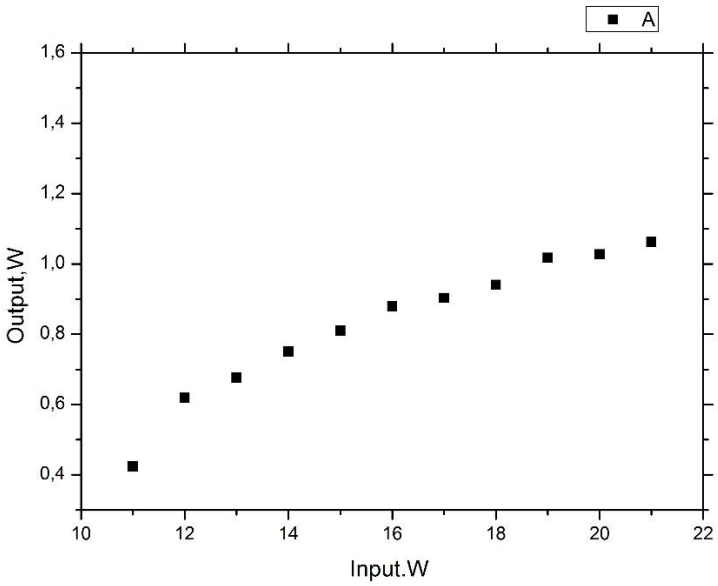

Figure 5.17: Balance of the VECSEL chips. First pump's power at threshold value, second pump's power is varying.

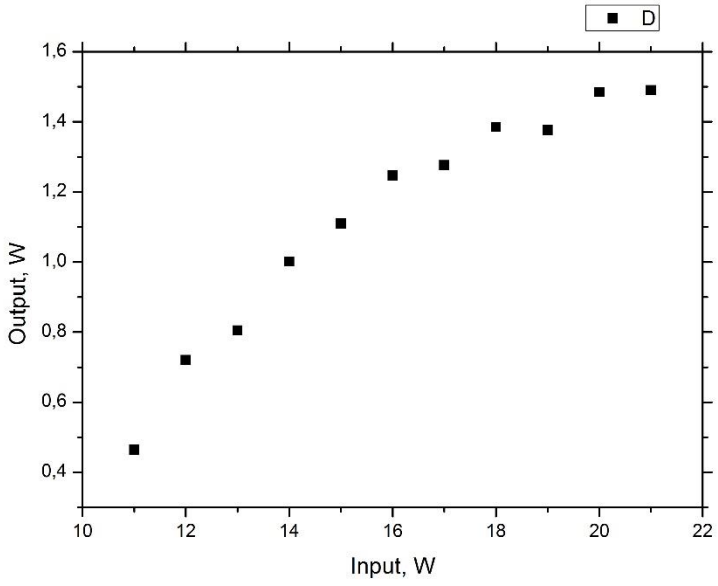

Figure 5.18: Balance of the VECSEL chips. Second pump's power at threshold value, first pump's power is varying

M^2 measurements of the single-chip setup are presented below.

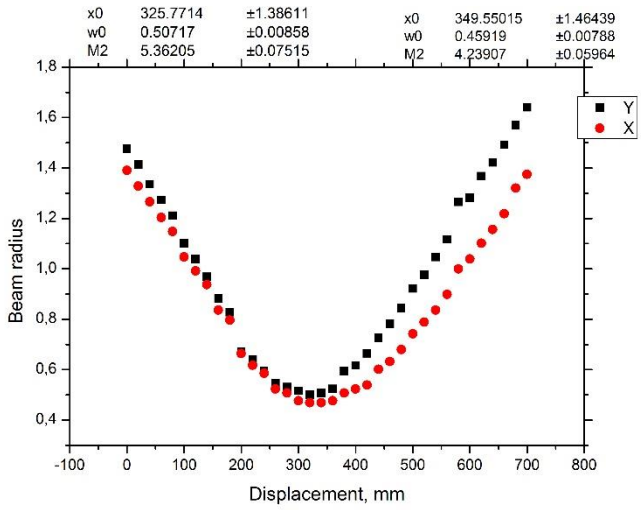

Figure 5.19: Experimental data fit for the deriving M^2 factor in the x and y-transversal-directions. The single-chip setup was equipped with the 2.5% OC.

As it can be seen M^2 is different for the different transversal directions. The presented M^2 factor can be considered as the relatively poor one, taking into account M^2 values ~1.5, characteristic for the most of VECSELs.

M^2 measurements of the multi-chip setup , done with two different output couplers.

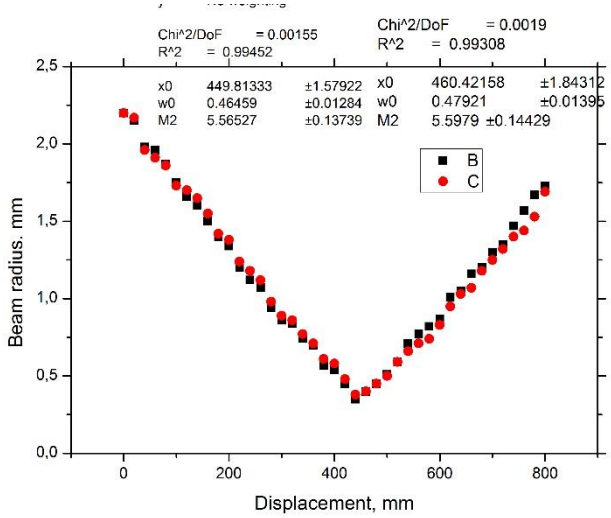

Figure 5.20: Experimental data fit for the deriving M^2 factor in the x and y-transversal-directions. The multi-chip setup was equipped with the 2.5 % OC.

The M^2 factors obtained by means of the measurements have poor values, which can be an evidence of the generation of high-order transverse modes, presence of which decreases the beam quality.

Polarization measurements of the laser output have been done.

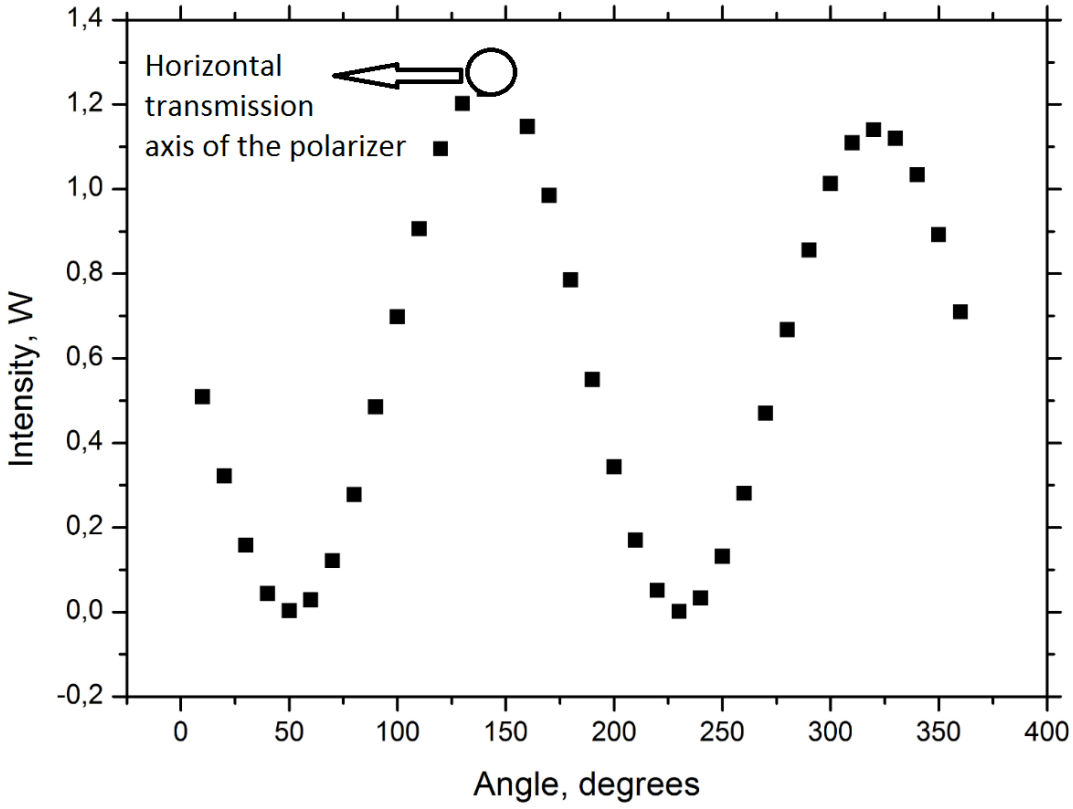

Figure 5.21: Polarization measurements. Measurements have been done by means of the rotation the polarizing cube and recording the output intensity. Angles of 140 and 320 degrees correspond to the horizontal axis of the polarizer. The 13 W of the pump power were applied.

The laser output light is s-polarized due to the multiple intracavity reflections from the beam splitter.

An attempt to combine two VECSEL chips with better spectrum matching was made. Only IC chips were available for this purpose.

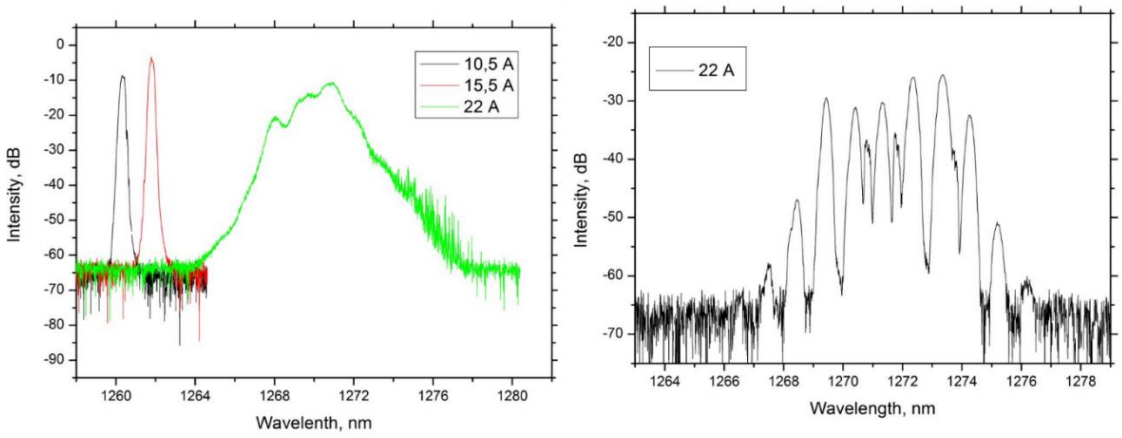

Figure 5.22: Spectra of the two IC VECSELs

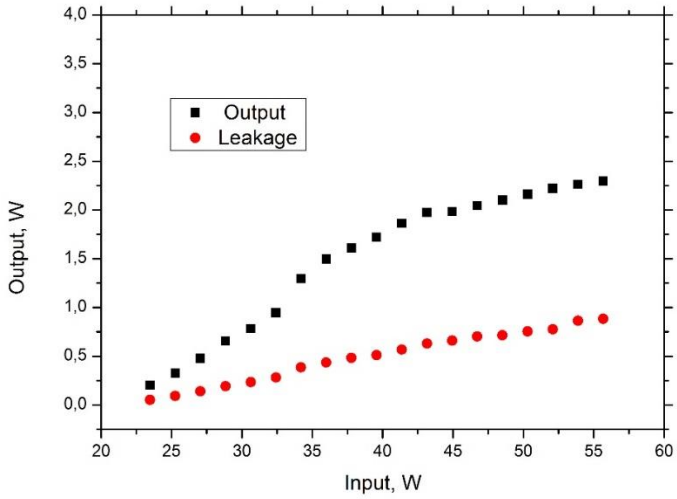

Figure 5.23: Power characteristics of the IC VECSEL multichip setup.

An attempt of building the interferometric setup with these two VECSELs in its core was not fully successful due to the several reasons. The first reason is that the chip's spectrum gets sufficiently broad only at high pumping powers. The same chip has a wedged diamond as an intracavity heat spreader. Reflection from the wedged diamond, nevertheless of AR coating, contributes to laser losses. The diamond of the second chip is not wedged, therefore it works as a Fabry-Perot etalon, which brings losses at some frequency modes. This fact might make impossible achieving frequency selection, in the case if q=0 mode will obtain additional losses from the diamond filtering effect. The power characteristics of the multi-chip also does not exceed the power characteristics of the single-chip setup.

Conclusion, discussion and further work

The sufficient theoretical background concerning VECSEL and descriptions of numerous interferometric designs and their applications have been provided. The first interferometric VECSEL has been built and investigated. Alignment techniques for building of the interferometric setup have been presented. Successful frequency selection of the laser output by means of frequency suppression technique in the Michelson-type interferometric cavity has been achieved.

For the author's point of view, the obtained results of the experimental work definitely assumes further improvements and modifications of the laser setup because desirable single-frequency operational mode has not been achieved, as well as efficient power combining of two VECSEL chips has not been achieved. First of all, proper VECSEL flip-chips should be selected. It means that VECSEL chips should have spectral coverage close to identical for better combining. VECSEL chips also should have bigger areas on its surface with satisfying performance. Second of all, laser setup has to be equipped with better mechanical part, i.e. more precise and stable translational and rotational mounts. Some principle changes can be implemented into interferometric design. For instance, the distance between VECSEL chips and beam splitter can be decreased in order to obtain bigger separation distance between transmission peaks. It can drastically simplify the frequency selection technique. Decreasing the length is linked to physical dimensions and placing of pump tubes and heatsinks, thus the positions of the pump tubes and their connections to the heatsink should be reconsidered. Different beam splitters can be further investigated in terms of this setup. Cooling system can be further changed to more efficient one.

All these improvements will bring closer the single-frequency operational regime and efficient power scaling. Single-frequency mode will open the possibility of a second-harmonic generation and obtaining the multi-watt single-frequency red laser beam, which will find a lot of applications

Bibliography

1. Maiman, Theodore (August 6, 1960). "Stimulated Optical Radiation in Ruby".Nature. 187 (4736): 493–94.
2. The early days of laser cutting, P. A. Hilton, 11th Nordic Conference in Laser Processing of Materials, Lappeenranta, Finland, August 20–22, 2007.
3. US 4784135, "Far ultraviolet surgical and dental procedures", issued 1988-10-15
4. Stan, Sorin G. (1998). The CD-ROM Drive: A Brief System Description. Springer. p. 13.
5. Alwayn, V. (2004). *Optical network design and implementation*. Indianapolis, IN: Cisco Press.
6. Buckley, Sean. "This Is How Valve's Amazing Lighthouse Tracking Technology Works". Gizmodo. Retrieved 2 July 2015.
7. Wikipedia. (2016). *Boeing YAL-1*. [online] Available at: https://en.wikipedia.org/wiki/Boeing_YAL-1 [Accessed 1 Aug. 2016].
8. *A NASA High-Power Space-Based Laser Research and Applications Program*. 1st ed. Washington D.C.: National Aeronautics and Space Administration. Available at: http://ntrs.nasa.gov/archive/nasa/casi.ntrs.nasa.gov/19830018929.pdf [Accessed 1 Aug. 2016].
9. M Nagatomo? and K Itoh?, 1991, "An evolutionary satellite power system for international demonstration in developing nations", SPS 91 Power from Space
10. A. Kantrowitz, in Proceedings of the International Conference on Lasers '87, F. J. Duarte, Ed. (STS Press, Mc Lean, VA, 1988)
11. Lubin, Philip (April 2015). "Effective Planetary Defense using Directed Energy". 4th IAA Planetary Defense Conference.
12. Patel, C. K. N. (1964). "Continuous-Wave Laser Action on Vibrational-Rotational Transitions of CO_2". Physical Review 136 (5A): A1187–
13. Moulton, P. (1986). Spectroscopic and laser characteristics of Ti:Al_2O_3. *Journal of the Optical Society of America B*, 3(1), p.125.

14. F. J. Duarte (Ed.), *Tunable Lasers Handbook* (Academic, New York, 1995) Chapter 9.
15. M. Kuznetsov *et al.*, "High-power (> 0.5-W CW) diode-pumped vertical-external-cavity surface-emitting semiconductor lasers with circular TEM_{00}beams", IEEE Photon. Technol. Lett. 9 (8), 1063 (1997)
16. Paschotta, D. (2016). *RP Photonics Consulting GmbH - technical consulting on laser technology, nonlinear optics, fiber optics; simulation and design software; encyclopedia and buyer's guide*. [online] Rp-photonics.com. Available at: https://www.rp-photonics.com [Accessed 1 Aug. 2016].
17. B. K. Garside and T. K. Lim, "Laser mode locking using saturable absorbers", J. Appl. Phys. 44 (5), 2335 (1973)
18. Okhotnikov, O. (2010). *Semiconductor disk lasers*. Weinheim: Wiley-VCH..
19. Coherent.com. (2016). *Laser Tools, Applications, Systems, Products, and Solutions | Coherent*. [online] Available at: http://www.coherent.com [Accessed 1 Aug. 2016].
20. Paschotta, D. (2016). *Encyclopedia of Laser Physics and Technology - laser diodes, semiconductor, gain, index guiding, high power*. [online] Rp-photonics.com. Available at: https://www.rp-photonics.com/laser_diodes.html [Accessed 1 Aug. 2016].
21. Sirbu, A., Rantamäki, A., Saarinen, E., Iakovlev, V., Mereuta, A., Lyytikäinen, J., Caliman, A., Volet, N., Okhotnikov, O. and Kapon, E. (2014). High performance wafer-fused semiconductor disk lasers emitting in the 1300 nm waveband. *Opt. Express*, 22(24), p.29398.
22. Paschotta, D. (2016). *Encyclopedia of Laser Physics and Technology - optical pumping, pump light, laser crystal, optically pumped lasers, pump absorption, in-band pumping*. [online] Rp-photonics.com. Available at: https://www.rp-photonics.com/optical_pumping.html?s=ak [Accessed 1 Aug. 2016].
23. Sokół, A. and Sarzała, R. (2013). Thermal management of GaInNAs/GaAs VECSELs. *Opto-Electronics Review*, 21(2).
24. Rantamäki, A. (2015). Scaling the Power and Tailoring the Wavelength of Semiconductor Disk Lasers. (Tampere University of Technology. Publication; Vol. 1286). Tampere University of Technology.

25. R. Bedford, M. Kolesik, J. Chilla, M. Reed, T. Nelson, and J. Moloney, “Powerlimiting mechanisms in VECSELs,” in Proceedings of SPIE, vol. 5814, 2005, pp. 199–208.
26. A. Zakharian, J. Hader, J. Moloney, and S. Koch, “VECSEL threshold and output power-shutoff dependence on the carrier recombination rates,” IEEE Photonics Technology Letters, vol. 17, no. 12, pp. 2511–2513, 2005.
27. S. Calvez, J. Hastie, M. Guina, O. Okhotnikov, and M. Dawson, “Semiconductor disk lasers for the generation of visible and ultraviolet radiation,” Laser & Photonics Reviews, vol. 3, no. 5, pp. 407–434, 2009.
28. Hariharan, P. (2007). *Basics of Interferometry*. Elsevier Inc. ISBN 0-12-373589-0
29. Feynman, R., Leighton, R. and Sands, M. (1963). *The Feynman lectures on physics*. Reading, Mass.: Addison-Wesley Pub. Co.
30. Shamos, Morris (1959). *Great Experiments in Physics*. New York: Holt Rinehart and Winston. pp. 96–101.
31. Greene, Brian (1999). *The Elegant Universe: Superstrings, Hidden Dimensions, and the Quest for the Ultimate Theory*. New York: W.W. Norton. pp. 97–109.ISBN 0-393-04688-5.
32. Ackermann, Gerhard K. (2007). *Holography: A Practical Approach*. Wiley-VCH. ISBN 3-527-40663-8.
33. Anderson, R.; Bilger, H.R.; Stedman, G.E. (1994). "Sagnac effect: A century of Earth-rotated interferometers". *Am. J. Phys.* **62** (11)
34. Sagnac, Georges (1913), "*L'éther lumineux démontré par l'effet du vent relatif d'éther dans un interféromètre en rotation uniforme*"
35. Michelson, Albert A.; Morley, Edward W. (1887). "On the Relative Motion of the Earth and the Luminiferous Ether". *American Journal of Science* **34**: 333–345.
36. Albert Einstein (1905) "*Zur Elektrodynamik bewegter Körper*", *Annalen der Physik* 17: 891; English translation On the Electrodynamics of Moving Bodies by George Barker Jeffery and Wilfrid Perrett (1923)
37. Norbert Wiener (1964). *Time Series*. M.I.T. Press, Cambridge, Massachusetts. p. 42.
38. Barish, Barry C.; Weiss, Rainer (October 1999). "LIGO and the Detection of Gravitational Waves". *Physics Today***52** (10): 44

39. LIGO Scientific Collaboration and Virgo Collaboration, B. P. Abbott (February 11, 2016). "Observation of Gravitational Waves from a Binary Black Hole Merger".*Physical Review Letters* **116** (6): 061102.
40. Ishaaya, A., Davidson, N. and Friesem, A. (2009). Passive Laser Beam Combining With Intracavity Interferometric Combiners. *IEEE J. Select. Topics Quantum Electron.*, 15(2), pp.301-311.A.Ishasya. Nir Davidson, A. Friesem, LIFE FELLOW, IEEE
41. Ishaaya, A., Eckhouse, V., Shimshi, L., Davidson, N. and Friesem, A. (2005). Improving the output beam quality of multimode laser resonators. *Opt. Express*, 13(7), p.2722.
42. Ishaaya, A., Davidson, N. and Friesem, A. (2009). Passive Laser Beam Combining With Intracavity Interferometric Combiners. *IEEE J. Select. Topics Quantum Electron.*, 15(2), pp.301-311.A.Ishasya. Nir Davidson, A. Friesem, LIFE FELLOW, IEEE
43. K. Kobayashi and I. Mito, "Single frequency and tunable laser diodes", J. Lightwave Technol. 6 (11), 1623 (1988)
44. H. Kogelnik and C. V. Shank, "Coupled-wave theory of distributed feedback lasers", J. Appl. Phys. 43 (5), 2327 (1972)
45. DiDomenico, M. (1966). Characteristics of a single-frequency Michelson-type He-Ne gas laser. *IEEE Journal of Quantum Electronics*, 2(8), pp.311-322.
46. Coherent, Inc., Santa Clara, CA, (2014). *MULTI-CHIP OPS-LASER*. US 2014/0016657 A1.
47. Thorlabs.com. (2016). *Thorlabs, Inc. - Your Source for Fiber Optics, Laser Diodes, Optical Instrumentation and Polarization Measurement & Control*. [online] Available at: https://www.thorlabs.com/ [Accessed 1 Aug. 2016].
48. Rantamäki, A, Sirbu, A, Saarinen, E, Lyytikäinen, J, Iakolev, V, Kapon, E & Okhotnikov, O 2014, 'High Power Wafer-Fused Flip Chip Semiconductor Disk Laser at 1.27 μm'. in *6th EPS-QEOD Europhoton Conference, 24-29 August, 2014, Neuchätel, Switzerland. Conference Digest: Europhysics Conference Abstract Volume 38 E*. EPS-QEOD Europhoton Conference, United Kingdom, 1 January.
49. O. Svetlo. *Principles of Lasers*. Plenum Press, New York, NY, 4th edition, 1998.
50. A.E. Siegman New developments in laser resonator. In *Proc.* SPIE 90, pages 2-14, 1990.